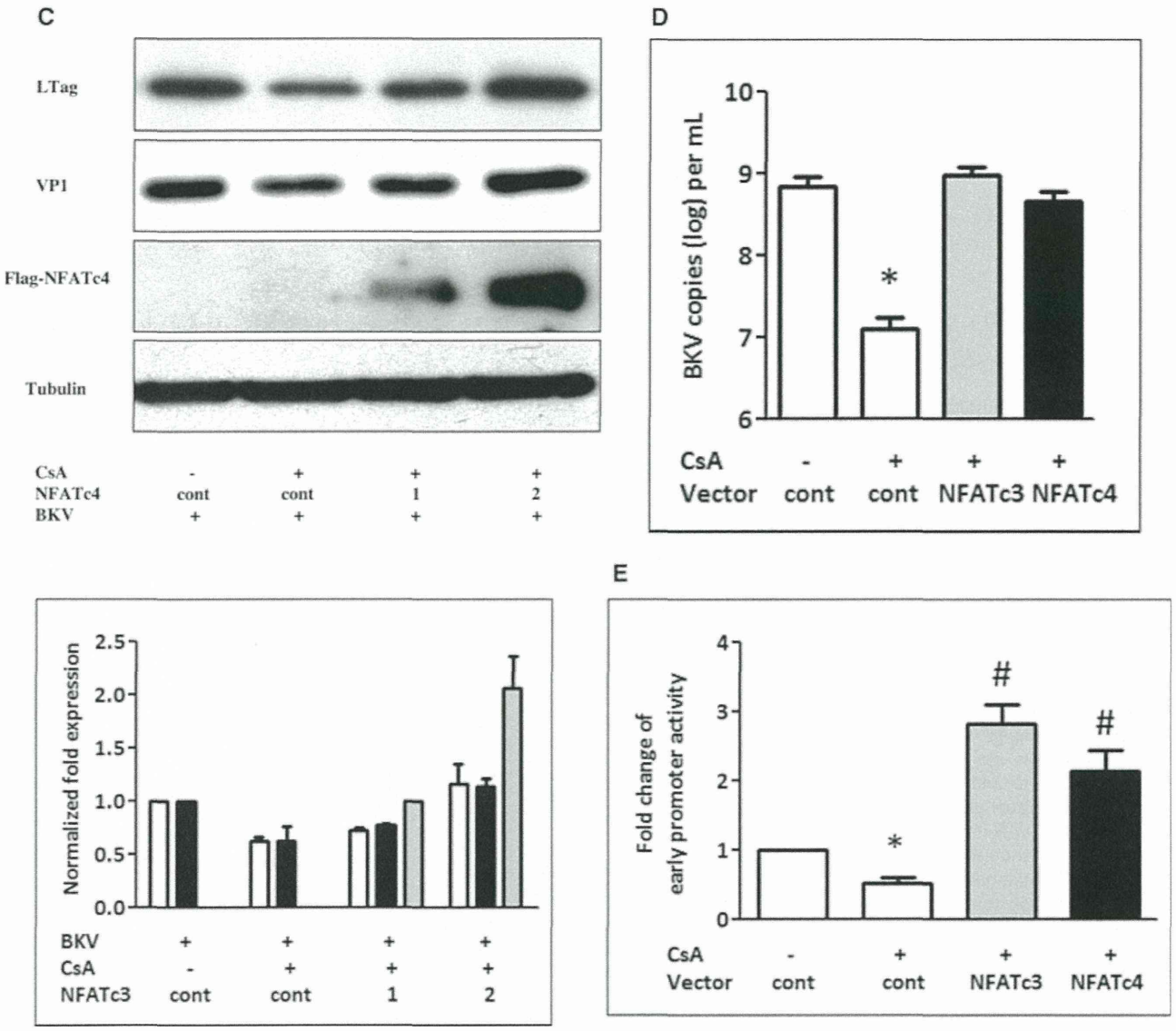

Figure 8: Continued

regulation of BKV transcription. The essential role of NFAT in viral replication has been reported in other viruses. Romanchikova et al. showed that NFATc1 and NFATc2 binding to HIV LTR enhanced HIV replication (37). Manley et al. have shown that NFATc3 is indispensable in JC virus (JCV) infection in glial cells as inhibition of NFATc3 by a NFAT peptide inhibitor reduced JCV promoter activity (38). In this study, renal histology of PVAN displayed an increase of NFATc3/c4 expression in renal tubules and lymphocytes. We speculate that increased NFATc3 expression in renal tubules may augment BKV replication and enhance the development of PVAN.

Previously we have shown that CsA can suppress BKV replication as the addition of CsA to the BKV-infected cells reduces BKV LTag expression (14). In this study, we further demonstrated that overexpression of CypA attenuated the suppressive effect of CsA on BKV TAg expression, which suggests anti-BKV effect of CsA requires inhibition of CypA activity. Several studies have demonstrated the essential role of cyclophilins in CsA-imposed inhibition of viral replication. Nakagawa et al. show that inhibition of HCV replication by CsA is through blockade of the activities of cyclophilins including CypA, CypB and CypC (29). Yang et al. also identified that CypA plays an essential

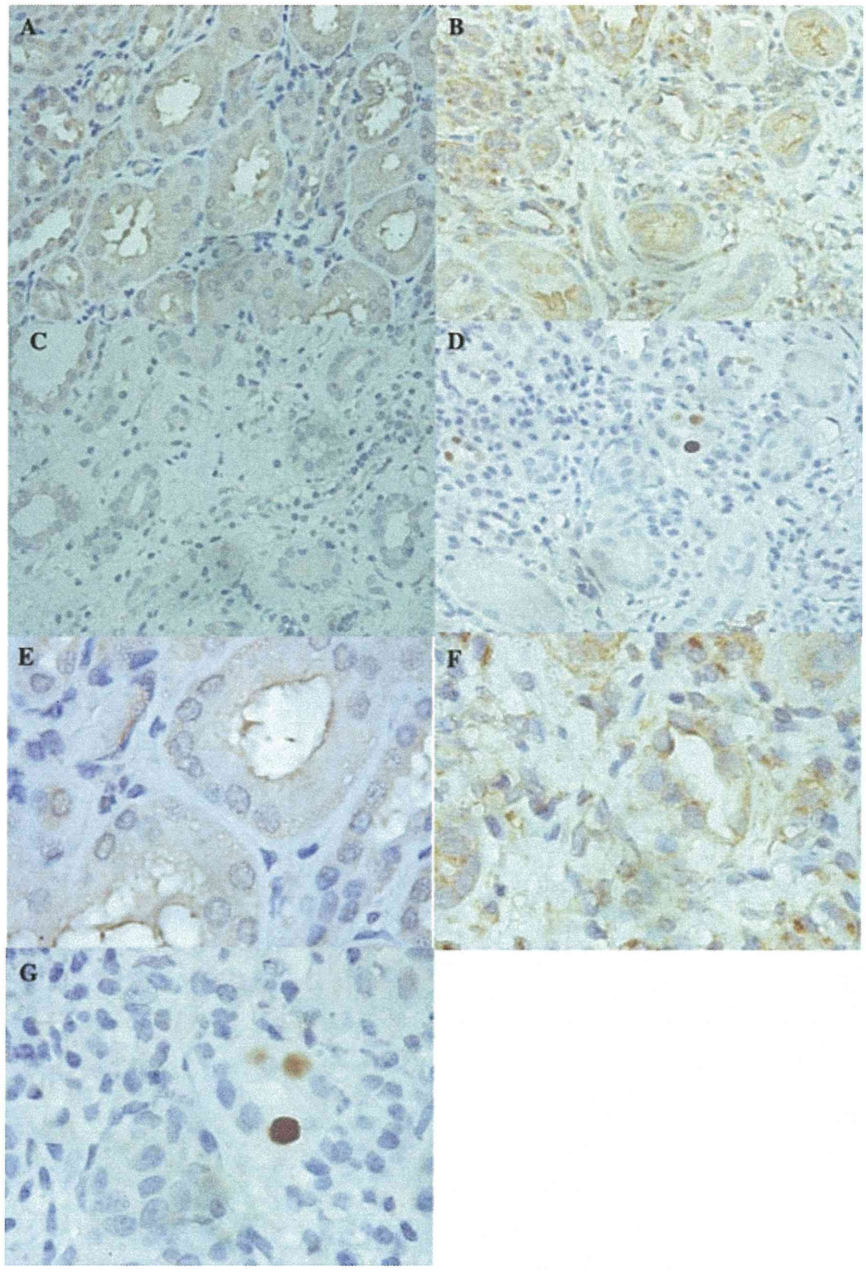

Figure 9: NFATc3 expression is increased in PVAN. NFATc3 expression (B and F, brown staining) and BKV TAg expression (D and G, dark brown staining) in the renal biopsy specimen obtained from PVAN patients were assessed by immunohistochemistry described in the Materials and Methods section. A negative control of the same specimen was performed using only the secondary antibody with omission of the primary antibody (anti-NFATc3) (C). Normal tissues cut from residual kidney specimen obtained from a nephrectomized patient with renal cell carcinoma were used as the control and stained for NFATc3 expression (A and E). Magnification: ABCD 400×, EFG 1000×.

role in CsA-resistant HCV infection (35). CypA is also a critical mediator in CsA-associated suppression of HIV, as the inhibitory effect of CsA on HIV replication results from CsA-induced disruption of the interaction between HIV Gag polyprotein and CypA (7). In accordance with these findings from other viruses, our results also suggest that CypA is critical for CsA-mediated suppression of BKV replication.

In this study, CsA, which caused phosphorylation of NFAT and inhibited NFAT activation, similar to the finding in COS-7 cells (39), suppressed BKV replication. In contrast, NIM811, which did not affect phosphorylation of NFAT and block NFAT functionality, failed to suppress BKV replication. Importantly, the overexpression of NFATc3 or NFATc4 attenuated the CsA-mediated inhibitory effect on BKV TAg expression. Moreover, NFATc3 or NFATc4 overexpression even surpassed the CsA-imposed reduction in the BKV early promoter activity. These findings indicate that NFAT is essential for the CsA-associated anti-BKV effect. It has been documented that CsA substantially interferes with the transcriptional activity of HIV mediated by NFAT in human CD4 T cells (22). Manely et al. report that CsA suppresses human polyomavirus JC (JCV) replication through

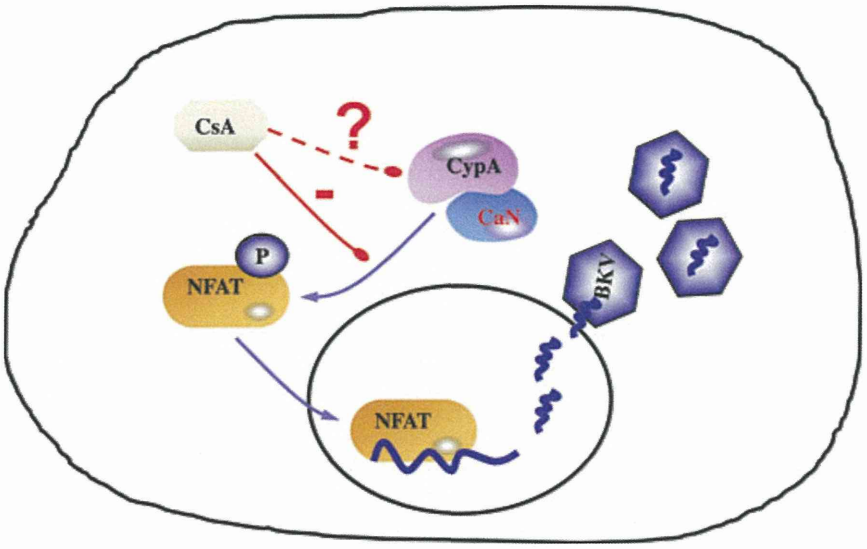

Figure 10: Schematic summary depicts a proposed mechanism of the inhibitory effect of CsA on BKV replication. NFATc3/c4, the calcineurin downstream mediator, can bind to the BKV NCCR to promoter viral replication. Administration of CsA blocks endogenous CypA/CaN function and leads to inhibition of dephosphorylation of NFAT, thus inhibiting NFAT functionality and preventing NFAT-mediated enhancement of BKV replication; CaN = calcineurin; CsA = cyclosporin; CypA = cyclophilin A; NFAT= nuclear factor of activated T cells.

blockade of NFAT4 activation (38). They identify a NFAT binding site as an enhancer in the early region of the JCV promoter, which is also conserved in the BKV promoter (38). In contrast, Jordan et al. identify three NFAT binding sites (GGAAA) in the triplicate P regions of the BKV Dunlop promoter and two of these are potential repressors (36). The BKV archetype strain also has three NFAT binding sites in the P, Q and R regions. Compared to the BKV archetype stain, the BKV TU strain has the rearranged NCCR containing the intact P- and Q-regions followed by a partial depletion of the R region and a duplication of a partial P–Q–R region (40). However, we also find three NFAT binding sites in the P, Q and R regions of the BKV TU promoter. Interestingly, despite the rearrangement of BKV NCCR, BKV archetype, Dunlop and TU strains all have three NFAT binding sites. Just which NFAT binding sites are the main regulatory sites in CsA-mediated suppression of BKV replication requires further elucidation.

The proposed mechanism regarding how CsA suppresses BKV replication is summarized in Figure 10. CypA is required in CsA-imposed inhibition of BKV replication since CypA overexpression can rescue this inhibitory response. In addition, NFATc3/c4, the calcineurin downstream mediator, can bind to the BKV NCCR to promoter viral replication. CsA, which blocks calcineurin activity, causes inhibition of dephosphorylation of NFAT, thus inhibiting NFAT functionality and preventing NFAT-mediated enhancement of BKV replication. Nevertheless, unlike CsA, knockdown of the CypA expression did not affect dephosphorylation of NFATc3 and the binding of NFATc3 to the BKV NCCR was not altered by administration of CypA siRNA (data not shown), suggesting an NFAT-independent role of CypA in BKV replication. Whether CsA also affects the CypA-dependent but NFAT-independent pathway (dash line in Figure 10) to regulate BKV replication requires further elucidation.

Several studies have demonstrated that tacrolimus, mycophenolic acid or steroids substantially increases the risk of BKV replication when compared with CsA (41–44) but it is the net immunosuppressive status of the host that determines the development of PVAN. Although CsA can suppress BKV replication in the *in vitro* culture, the rationality of shifting to CsA-based immunosuppressants in renal transplant patients with PVAN still remains controversial due to side effects including nephrotoxicity and development of renal fibrosis (45). Since calcineurin/cyclophilin has functional diversity in regulating cell bio-functions and dephophorylates not only NFAT but also many intracellular proteins (17), CsA therefore blocks NFAT functionality as well as other important cell biological activities (46). Specific therapeutic agents targeting against CypA and NFAT may provide new potential anti-BKV treatment.

In conclusion, this study demonstrates an essential role of CypA and NFATc3 in BKV replication. CsA suppresses BKV replication through inhibition of CypA and NFAT functionalities.

Acknowledgments

This study was supported by grants (NMRPD190372, NMRPG596042) from the National Science Council of Taiwan and grants (CMRPG381062, CMRPG390921) from the Chung Gang Medical Research Project to Dr. Y.-C.T. and Dr. I.-J.L.

Disclosure

The authors of this manuscript have no conflicts of interest to disclose as described by the *American Journal of Transplantation*.

References

1. Hirsch HH, Drachenberg CB, Steiger J, Ramos E. Polyomavirus-associated nephropathy in renal transplantation: Critical issues of screening and management. Adv Exp Med Biol 2006; 577: 160–173.
2. Li YJ, Chen YC, Lai PC, et al. A direct association of polyomavirus BK viruria with deterioration of renal allograft function in renal transplant patients. Clin Transplant 2009; 23: 505–510.
3. Hirsch HH, Brennan DC, Drachenberg CB, et al. Polyomavirus-associated nephropathy in renal transplantation: Interdisciplinary analyses and recommendations. Transplantation 2005; 79: 1277–1286.
4. BK virus. Am J Transplant 2004; 4(Suppl 10): 89–91.
5. Agha I, Brennan DC. BK virus and immunosuppressive agents. Adv Exp Med Biol 2006; 577: 174–184.
6. Brennan DC, Agha I, Bohl DL, et al. Incidence of BK with tacrolimus versus cyclosporine and impact of preemptive immunosuppression reduction. Am J Transplant 2005; 5: 582–594.
7. Franke EK, Luban J. Inhibition of HIV-1 replication by cyclosporine A or related compounds correlates with the ability to disrupt the Gag-cyclophilin A interaction. Virology 1996; 222: 279–282.
8. Damaso CR, Keller SJ. Cyclosporin A inhibits vaccinia virus replication in vitro. Arch Virol 1994; 134: 303–319.
9. Vahlne A, Larsson PA, Horal P, et al. Inhibition of herpes simplex virus production in vitro by cyclosporin A. Arch Virol 1992; 122: 61–75.
10. Wainberg MA, Dascal A, Blain N, et al. The effect of cyclosporine A on infection of susceptible cells by human immunodeficiency virus type 1. Blood 1988; 72: 1904–1910.
11. Kawasaki H, Mocarski ES, Kosugi I, Tsutsui Y. Cyclosporine inhibits mouse cytomegalovirus infection via a cyclophilin-dependent pathway specifically in neural stem/progenitor cells. J Virol 2007; 81: 9013–9023.
12. Watashi K, Hijikata M, Hosaka M, Yamaji M, Shimotohno K. Cyclosporin A suppresses replication of hepatitis C virus genome in cultured hepatocytes. Hepatology 2003; 38: 1282–1288.
13. Acott PD, O'Regan PA, Lee SH, Crocker JF. In vitro effect of cyclosporin A on primary and chronic BK polyoma virus infection in Vero E6 cells. Transpl Infect Dis 2008; 10: 385–390.
14. Li YJ, Weng CH, Lai WC, et al. A suppressive effect of cyclosporine A on replication and noncoding control region activation of polyomavirus BK virus. Transplantation 2010; 89: 299–306.
15. Handschumacher RE, Harding MW, Rice J, Drugge RJ, Speicher DW. Cyclophilin: A specific cytosolic binding protein for cyclosporin A. Science 1984; 226: 544–547.
16. Wang P, Heitman J. The cyclophilins. Genome Biol 2005; 6: 226.
17. Matsuda S, Koyasu S. Mechanisms of action of cyclosporine. Immunopharmacology 2000; 47: 119–125.
18. Ho S, Clipstone N, Timmermann L, et al. The mechanism of action of cyclosporin A and FK506. Clin Immunol Immunopathol 1996; 80(3 Pt 2): S40–S45.
19. Hogan PG, Chen L, Nardone J, Rao A. Transcriptional regulation by calcium, calcineurin, and NFAT. Genes Dev 2003; 17: 2205–2232.
20. Crabtree GR. Generic signals and specific outcomes: Signaling through Ca2+, calcineurin, and NF-AT. Cell 1999; 96: 611–614.
21. Chatterji U, Bobardt M, Selvarajah S, et al. The isomerase active site of cyclophilin A is critical for hepatitis C virus replication. J Biol Chem 2009; 284: 16998–17005.
22. Cron RQ, Bartz SR, Clausell A, Bort SJ, Klebanoff SJ, Lewis DB. NFAT1 enhances HIV-1 gene expression in primary human CD4 T cells. Clin Immunol 2000; 94: 179–191.
23. Tian YC, Chen YC, Chang CT, et al. Epidermal growth factor and transforming growth factor-beta1 enhance HK-2 cell migration through a synergistic increase of matrix metalloproteinase and sustained activation of ERK signaling pathway. Exp Cell Res 2007; 313: 2367–2377.
24. Goel M, Sinkins WG, Schilling WP. Selective association of TRPC channel subunits in rat brain synaptosomes. J Biol Chem 2002; 277: 48303–48310.
25. Tian YC, Hung CC, Li YJ, et al. Leptospira santorosai serovar shermani detergent extract induces an increase in fibronectin production through a toll-like receptor 2-mediated pathway. Infect Immun 2011; 79: 1134–1142.
26. Tian YC, Phillips AO. TGF-beta1-mediated inhibition of HK-2 cell migration. J Am Soc Nephrol 2003; 14: 631–640.
27. Moriyama T, Sorokin A. BK virus (BKV): Infection, propagation, quantitation, purification, labeling, and analysis of cell entry. Curr Protoc Cell Biol 2009;Chapter 26:Unit 26 2.
28. Watashi K, Ishii N, Hijikata M, et al. Cyclophilin B is a functional regulator of hepatitis C virus RNA polymerase. Mol Cell 2005; 19: 111–122.
29. Nakagawa M, Sakamoto N, Tanabe Y, et al. Suppression of hepatitis C virus replication by cyclosporin a is mediated by blockade of cyclophilins. Gastroenterology 2005; 129: 1031–1041.
30. Jain J, McCaffrey PG, Miner Z, et al. The T-cell transcription factor NFATp is a substrate for calcineurin and interacts with Fos and Jun. Nature 1993; 365: 352–355.
31. Martinez-Martinez S, Redondo JM. Inhibitors of the calcineurin/NFAT pathway. Curr Med Chem 2004; 11: 997–1007.
32. Liu S, Asparuhova M, Brondani V, Ziekau I, Klimkait T, Schumperli D. Inhibition of HIV-1 multiplication by antisense U7 snRNAs and siRNAs targeting cyclophilin A. Nucleic Acids Res 2004; 32: 3752–3759.
33. Chatterji U, Bobardt M, Lim P, Gallay P. Cyclophilin A-Independent Recruitment of NS5A and NS5B Into HCV Replication Complexes. J Gen Virol 2010; 91: 1189–1193.
34. Kaul A, Stauffer S, Berger C, et al. Essential role of cyclophilin A for hepatitis C virus replication and virus production and possible link to polyprotein cleavage kinetics. PLoS Pathog 2009; 5: e1000546.
35. Yang F, Robotham JM, Nelson HB, Irsigler A, Kenworthy R, Tang H. Cyclophilin A is an essential cofactor for hepatitis C virus infection and the principal mediator of cyclosporine resistance in vitro. J Virol 2008; 82: 5269–5278.
36. Jordan JA, Manley K, Dugan AS, O'Hara BA, Atwood WJ. Transcriptional regulation of BK virus by nuclear factor of activated T cells. J Virol 2010; 84: 1722–1730.
37. Romanchikova N, Ivanova V, Scheller C, Jankevics E, Jassoy C, Serfling E. NFAT transcription factors control HIV-1 expression through a binding site downstream of TAR region. Immunobiology 2003; 208: 361–365.
38. Manley K, O'Hara B A, Gee GV, Simkevich CP, Sedivy JM, Atwood WJ. NFAT4 is required for JC virus infection of glial cells. J Virol 2006; 80: 12079–12085.
39. Trevillyan JM, Chiou XG, Chen YW, et al. Potent inhibition of NFAT activation and T cell cytokine production by novel low molecular weight pyrazole compounds. J Biol Chem 2001; 276: 48118–48126.
40. Sundsfjord A, Johansen T, Flaegstad T, et al. At least two types of control regions can be found among naturally occurring BK virus strains. J Virol 1990; 64: 3864–3871.
41. Barri YM, Ahmad I, Ketel BL, et al. Polyoma viral infection in renal transplantation: The role of immunosuppressive therapy. Clin Transplant 2001; 15: 240–246.

42. Binet I, Nickeleit V, Hirsch HH, et al. Polyomavirus disease under new immunosuppressive drugs: A cause of renal graft dysfunction and graft loss. Transplantation 1999; 67: 918–922.
43. Dadhania D, Snopkowski C, Ding R, et al. Epidemiology of BK virus in renal allograft recipients: Independent risk factors for BK virus replication. Transplantation 2008; 86: 521–528.
44. Nickeleit V, Hirsch HH, Binet IF, et al. Polyomavirus infection of renal allograft recipients: From latent infection to manifest disease. J Am Soc Nephrol 1999; 10: 1080–1089.
45. Chapman JR, Nankivell BJ. Nephrotoxicity of ciclosporin A: Short-term gain, long-term pain? Nephrol Dial Transplant 2006; 21: 2060–2063.
46. Akool el S, Doller A, Babelova A, et al. Molecular mechanisms of TGF beta receptor-triggered signaling cascades rapidly induced by the calcineurin inhibitors cyclosporin A and FK506. J Immunol 2008; 181: 2831–2845.

Antimicrobial Agents and Chemotherapy

Identification of Novel *N*-(Morpholine-4-Carbonyloxy) Amidine Compounds as Potent Inhibitors against Hepatitis C Virus Replication

Akiko Kusano-Kitazume, Naoya Sakamoto, Yukiko Okuno, Yuko Sekine-Osajima, Mina Nakagawa, Sei Kakinuma, Kei Kiyohashi, Sayuri Nitta, Miyako Murakawa, Seishin Azuma, Yuki Nishimura-Sakurai, Masatoshi Hagiwara and Mamoru Watanabe

Antimicrob. Agents Chemother. **2012, 56(3):1315. DOI: 10.1128/AAC.05764-11.**
Published Ahead of Print 27 December 2011.

AAC
Journals.ASM.org

Identification of Novel *N*-(Morpholine-4-Carbonyloxy) Amidine Compounds as Potent Inhibitors against Hepatitis C Virus Replication

Akiko Kusano-Kitazume,[a] Naoya Sakamoto,[a,b] Yukiko Okuno,[c] Yuko Sekine-Osajima,[a] Mina Nakagawa,[a,b] Sei Kakinuma,[a,b] Kei Kiyohashi,[a] Sayuri Nitta,[a] Miyako Murakawa,[a] Seishin Azuma,[a] Yuki Nishimura-Sakurai,[a] Masatoshi Hagiwara,[c] and Mamoru Watanabe[a]

Department of Gastroenterology and Hepatology[a] and Department for Hepatitis Control,[b] Tokyo Medical and Dental University, Tokyo, Japan, and Department of Anatomy and Developmental Biology, Graduate School of Medicine, Kyoto University, Kyoto, Japan[c]

To identify novel compounds that possess antiviral activity against hepatitis C virus (HCV), we screened a library of small molecules with various amounts of structural diversity using an HCV replicon-expressing cell line and performed additional validations using the HCV-JFH1 infectious-virus cell culture. Of 4,004 chemical compounds, we identified 4 novel compounds that suppressed HCV replication with 50% effective concentrations of ranging from 0.36 to 4.81 μM. *N*′-(Morpholine-4-carbonyloxy)-2-(naphthalen-1-yl) acetimidamide (MCNA) was the most potent and also produced a small synergistic effect when used in combination with alpha interferon. Structure-activity relationship (SAR) analyses revealed 4 derivative compounds with antiviral activity. Further SAR analyses revealed that the *N*-(morpholine-4-carbonyloxy) amidine moiety was a key structural element for antiviral activity. Treatment of cells with MCNA activated nuclear factor κB and downstream gene expression. In conclusion, *N*-(morpholine-4-carbonyloxy) amidine and other related morpholine compounds specifically suppressed HCV replication and may have potential as novel chemotherapeutic agents.

Hepatitis C virus (HCV) is a major human pathogen. It is associated with persistent liver infection, which leads to the development of chronic hepatitis, liver cirrhosis, and hepatocellular carcinoma (13). Treatment with pegylated interferon (IFN) and ribavirin is associated with significant side effects and is effective in only half the patients infected with HCV genotype 1 (6). More effective and more tolerable therapeutics are under development, and direct-acting antiviral agents (DAAs) for HCV infection are currently in advanced clinical trials. In combination with IFN and ribavirin, the HCV protease inhibitors telaprevir and boceprevir have recently been approved for treatment of genotype 1 HCV infection in the United States, Canada, Europe, and Asian countries (11, 12, 22). Although these two drugs can achieve higher sustained virologic response rates than IFN and ribavirin, their effects could be compromised by the emergence of highly prevalent drug-resistant mutants (25). Thus, it is crucial to use several different classes of DAAs in combination to improve efficacy and reduce viral breakthrough.

The HCV subgenomic replicon system has been widely used to screen compound libraries for inhibitors of viral replication, using reporter activity as a surrogate marker for HCV replication. We previously reported the successful adaptation of the Huh7/Rep-Feo replicon cell line to a high-throughput screening assay system (28). This approach contributed to the discovery of antiviral compounds, such as hydroxyl-methyl-glutaryl coenzyme A reductase inhibitors (10) and epoxide compounds (20). In our present study, we used the Huh7/Rep-Feo replicon cell line to screen a library of small molecules with various amounts of structural diversity to identify novel compounds possessing antiviral activity against HCV. We showed that the screening hit compounds inhibited HCV replication in an HCV genotype 2a (JFH-1) infectious-virus cell culture (29). The most potent compound was *N*′-(morpholine-4-carbonyloxy)-2-(naphthalen-1-yl) acetimidamide (MCNA). Structure-activity relationship (SAR) analyses revealed that the *N*-(morpholine-4-carbonyloxy) amidine moiety was a key structural element for antiviral activity. We also investigated the possible mechanisms of action of these compounds and showed that MCNA likely inhibited HCV replication through activation of the nuclear factor κB (NF-κB) pathway.

MATERIALS AND METHODS

Reagents and chemicals. Recombinant human alpha 2b interferon (IFN-α2b) was obtained from Schering-Plough (Kenilworth, NJ), the NS3/4A protease inhibitor BILN 2061 from Boehringer Ingelheim (Ingelheim, Germany), beta-mercaptoethanol from Wako (Osaka, Japan), and recombinant human tumor necrosis factor alpha (TNF-α) from Sigma (St. Louis, MO). The library of chemicals that were screened was provided by the Chemical Biology Screening Center at Tokyo Medical and Dental University. Information about the library is available at http://bsmdb.tmd.ac.jp. The important features of the library were the abundance of pharmacophores and the great diversity. Lipinski's rule of five was used to evaluate drug similarity (15). The purity of each chemical from the library was greater than 90%. For SAR analyses, 27 compounds were purchased from Assinex (Moscow, Russia), ChemBridge (San Diego, CA), ChemDiv (San Diego, CA), Enamine (Kiev, Ukraine), Maybridge (Cambridge, United Kingdom), Ramidus AB (Lund, Sweden), SALOR (St. Louis, MO), Scientific Exchange (Center Ossipee, NH), or Vitas-M (Moscow, Russia). The chemicals were all prepared at concentrations of 10 mM in dimethyl sulfoxide (Sigma) and stored at −20°C until they were used.

Cell lines and cell culture maintenance. Huh7 and Huh7.5.1 cell lines (32) were maintained in Dulbecco's modified Eagle's medium (Sigma)

Received 22 September 2011 Returned for modification 18 October 2011
Accepted 14 December 2011
Published ahead of print 27 December 2011
Address correspondence to Naoya Sakamoto, nsakamoto.gast@tmd.ac.jp.
A. Kusano-Kitazume and N. Sakamoto contributed equally to this work.
Supplemental material for this article may be found at http://aac.asm.org/.

doi:10.1128/AAC.05764-11

supplemented with 10% fetal bovine serum and incubated at 37°C under 5% CO_2. The maintenance medium for the HCV replicon-harboring cell line, Huh7/Rep-Feo, was supplemented with 500 μg/ml of G418 (Nacalai Tesque, Kyoto, Japan).

HCV replicon construction and cell culture. An HCV subgenomic replicon plasmid that contained Rep-Feo, pHC1bneo/delS (Rep-Feo-1b), was derived from the HCV-N strain. RNA was synthesized from pRep-Feo and transfected into Huh7 cells. After culture in the presence of G418, a cell line that stably expressed the replicon was established (28, 31).

Cell-based screening of antiviral activity. Huh7/Rep-Feo cells were seeded at a density of 4,000 cells/well in 100 μl of medium in 96-well plates and incubated for 24 h. Test compound solutions, 10 mM in 100% dimethyl sulfoxide (DMSO), were added to the wells; for primary screening, the final concentration was 5 μM. The assay plates were incubated as described above for another 48 h, and luciferase activity was measured with a luminometer (Perkin-Elmer) using the Bright-Glo Luciferase assay system (Promega) following the manufacturer's instructions. Assays were performed in triplicate, and the results were expressed as means and standard deviations (SD) as percentages of the controls. Compounds were considered hits if they inhibited >50% of the mean control luciferase activities. Compounds were considered cytotoxic if they reduced cell viability below 70% of the control in dimethylthiazol carboxymethoxyphenyl sulfophenyl tetrazolium (MTS) assays and were discarded. The hit compounds were then validated by secondary screening, which determined the antiviral activities of each compound serially diluted at concentrations ranging from 0.1 μM to 30 μM under Huh7/Rep-Feo cells cultured in an identical manner to the primary screen. Compounds inhibiting replication with a 50% effective concentration (EC_{50}) of <5 μM and a selectivity index (SI) of >5 were selected for further analysis.

MTS assay. To evaluate cell viability, MTS assays were performed using the CellTiter 96 Aqueous One Solution Cell Proliferation Assay (Promega) according to the manufacturer's directions.

Calculation of the EC_{50}, CC_{50}, and SI. The EC_{50} indicates the concentration of test compound that inhibits replicon-based luciferase activity by 50%. The 50% cytotoxic concentration (CC_{50}) indicates the concentration that inhibits cell viability by 50%. The EC_{50} and CC_{50} values were calculated using probit regression analysis (2, 26). The selectivity index was calculated by dividing the CC_{50} by the EC_{50}.

Reporter and expression plasmids. The plasmid pC1neo-Rluc-IRES-Fluc was constructed to analyze the HCV internal ribosome entry site (IRES)-mediated translation efficiency (19). The plasmid expressed a bicistronic mRNA containing the *Renilla* luciferase gene translated in a cap-dependent manner, and firefly luciferase was translated by HCV-IRES-mediated initiation. The plasmid pISRE-TA-Luc (Invitrogen, Carlsbad, CA) expressed the firefly luciferase reporter gene under the control of the interferon stimulation response element (ISRE). The plasmid pNF-κB-TA-Luc (Clontech Laboratories, Franklin Lakes, NJ) expressed the firefly luciferase reporter gene under the control of NF-κB. The plasmid pRL-CMV (Promega, Madison, WI), which expressed the *Renilla* luciferase gene under the control of the cytomegalovirus early promoter/enhancer, was used as a control for the transfection efficiency of pISRE-TA-Luc and pNF-κB-TA-Luc (8).

Western blot analysis. Fifteen micrograms of total cell lysates was separated using NuPage 4-to-12% Bis-Tris gels (Invitrogen) and blotted onto polyvinylidene difluoride membranes. Each membrane was incubated with primary antibodies followed by a peroxidase-labeled anti-IgG antibody and visualized by chemiluminescence reaction using the ECL Western Blotting Analysis System (Amersham Biosciences, Buckinghamshire, United Kingdom). The primary antibodies were anti-NS5A (BioDesign, Saco, ME), anti-HCV core (kindly provided by T. Wakita), anti-phospho-p65 (Ser536) (93H1; Cell Signaling Technology, Beverly, MA), anti-IκBα (Santa Cruz Biotechnology, Santa Cruz, CA), and anti-β-actin (Sigma) antibodies.

HCV-JFH1 virus cell culture. HCV-JFH1 RNA transcribed *in vitro* was transfected into Huh7.5.1 cells. The transfected cells were subcultured every 3 to 5 days. The culture supernatant was subsequently transferred onto Huh7.5.1 cells.

TABLE 1 Effects of the leading hit compounds on HCV replication[a]

Compound	EC_{50} (μM)	CC_{50} (μM)	SI
1	0.36 (0.22–0.58)	45.2 (35.9–56.9)	126
2	0.86 (0.73–1.02)	>100	>116
3	0.94 (0.76–1.06)	25.3 (19.8–32.3)	26.9
4	4.81 (3.79–6.12)	27.1 (17.1–58.0)	5.64

[a] The EC_{50} and CC_{50} values are reported, with 95% confidence intervals in parentheses, from a representative experiment performed in triplicate.

Real-time RT-PCR analysis. The protocols and primers for real-time RT-PCR analysis of HCV RNA have been described previously (17). Briefly, total cellular RNA was isolated using an RNeasy Minikit (Qiagen, Valencia, CA), reverse transcribed, and subjected to real-time RT-PCR analysis. Expression of mRNA was quantified using the TaqMan Universal PCR Master Mix (Applied Biosystems, Foster City, CA) and the ABI 7500 real-time PCR system (Applied Biosystems).

Analyses of drug synergism. The effects on HCV replication of antiviral hit compounds plus IFN-α or BILN 2061 were analyzed according to classical isobologram analyses (24, 28). Dose-inhibition curves for IFN or BILN 2061 and the test compounds were drawn, with the 2 drugs (IFN or BILN 2061 and each test compound) used alone or in combination. For each drug combination, the concentrations of IFN or BILN 2061 and test compound that inhibited HCV replication by 50% (EC_{50}s) were plotted against the fractional concentration of IFN or BILN 2061 and the compound on the *x* and *y* axes, respectively. A theoretical line of additivity was drawn between plots of the EC_{50}s obtained for either drug used alone. The combined effects of the 2 drugs were considered to be additive, synergistic, or antagonistic if the plots of the combined drugs were located on, below, or above the line of additivity, respectively.

Statistical analyses. Statistical analyses were performed using Welch's *t* test. *P* values of less than 0.01 were considered statistically significant.

RESULTS

Screening results. To identify novel regulators of HCV replication, 4,004 chemical compounds were screened using the Huh7/Rep-Feo replicon assay system. The primary screens identified 117 compounds that inhibited ≥50% of replicon luciferase activity at 5 μM. Of the 117 compounds, 74 were cytotoxic and could not be further evaluated. In the secondary screen, nontoxic primary hits were evaluated by determining the antiviral activities of serial dilutions at concentrations ranging from 0.1 μM to 30 μM. This screen identified 19 compounds with EC_{50}s of less than 5 μM and CC_{50} values 5-fold greater than the EC_{50} values. The effect of each secondary hit on HCV-NS5A protein expression was examined using Western blot analysis. Of the 19 compounds, 4 compounds, designated 1, 2, 3, and 4, suppressed HCV subgenomic replication, with EC_{50}s ranging from 0.36 to 4.81 μM and SIs ranging from 5.64 to more than 100 (Table 1 and Fig. 1A and B; see Table S1 in the supplemental material). By Western blot analysis, compounds 1, 2, and 3 decreased HCV-NS5A protein levels at concentrations of 5 μM after incubation for 48 h (Fig. 1C). Compared with compounds 1, 2, and 3, the effect of compound 4 on HCV-NS5A protein expression was not remarkable at a concentration of 5 μM, similar to the results from the luciferase assay shown in Fig. 1B. The effects of the compounds on the HCV replicon were further validated in the JFH-1 cell culture. As shown in Fig. 1D, compounds 1, 2, 3, and 4 significantly inhibited intracellular RNA replication of HCV-JFH1. Although compound 4 was negative by Western blot analysis, it decreased HCV replication in the other

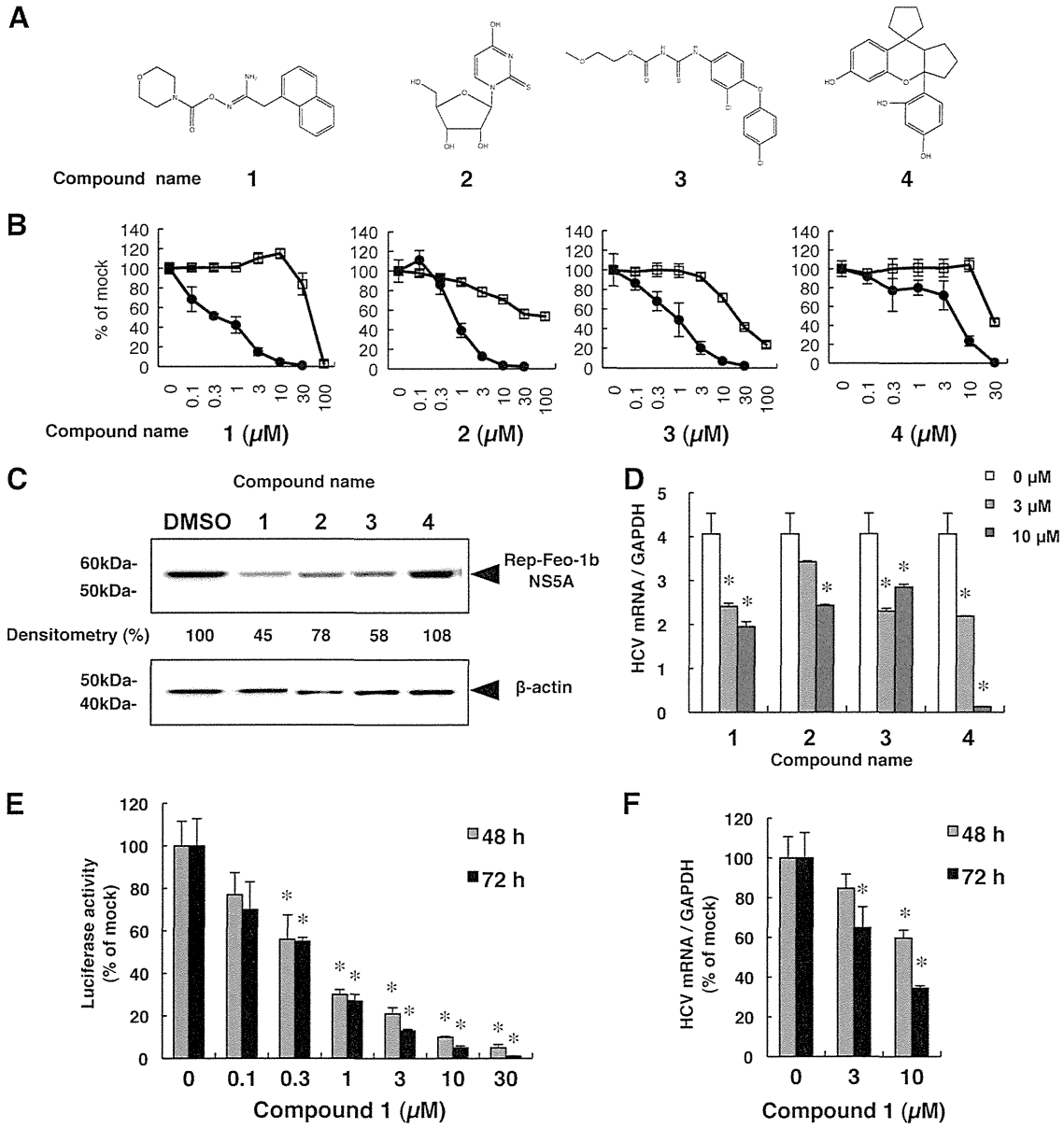

FIG 1 Effects of 4 screening hit compounds on HCV replication. (A) Chemical structures of hit compounds. (B) Huh7/Rep-Feo cells were treated with the indicated concentration of each compound for 48 h. Luciferase activities representing HCV replication are shown as percentages of the DMSO-treated control luciferase activity (solid circles). Cell viability is shown as a percentage of control viability (open squares). Each point represents the mean of triplicate data points, with the standard deviations represented as error bars. (C) Huh7/Rep-Feo cells were treated with DMSO or compounds 1 through 4 at 5 μM for 48 h, and Western blotting was performed using anti-HCV NS5A and anti-β-actin antibodies. Densitometry of NS5A protein was performed, and the results are indicated as percentages of the DMSO-treated control. The assay was repeated three times, and a representative result is shown. (D) Huh7.5.1 cells were transfected with HCV-JFH1 RNA and cultured in the presence of the indicated compounds at 3 μM or 10 μM. At 72 h after transfection, the cellular expression levels of HCV-RNA were quantified by real-time RT-PCR. The bars indicate means and SD. (E) Time-dependent reduction of luciferase activities in Huh7/Rep-Feo cells induced by compound 1. Luciferase activities are shown as percentages of the DMSO-treated control luciferase activity. The bars indicate means and SD. (F) Time-dependent reduction of cellular expression levels of HCV-RNA in HCV-JFH1-transfected cells induced by compound 1. HCV RNA levels are shown as percentages of the DMSO-treated control HCV-RNA level. The bars indicate means and SD. The asterisks indicate P values of less than 0.01.

assays, including the replicon and HCV-JFH1 virus assays. Thus, we concluded that compound 4 was an antiviral hit. These results indicated that the 4 compounds identified by cell-based screening suppressed subgenomic HCV replication and HCV replication in an HCV-based cell culture.

Hit compounds did not suppress HCV IRES-mediated translation. To determine whether the leading antiviral hits suppressed HCV IRES-dependent translation, we used the Huh7 cell line that had been stably transfected with pCIneo-Rluc IRES-Fluc. Treatment of these cells with the test compounds did not result in significant change in the internal luciferase activities at compound concentrations that suppressed expression of the HCV replicon (Fig. 2), suggesting that the effect of the hit compounds on HCV replication does not involve suppression of IRES-mediated viral-protein synthesis.

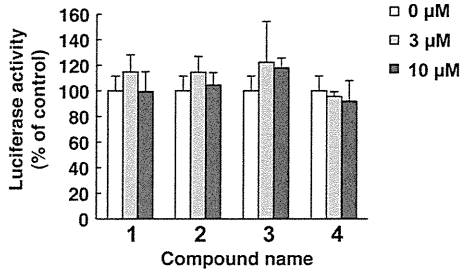

FIG 2 Hit compounds do not affect HCV IRES-mediated translation. The bicistronic reporter plasmid pC1neo-Rluc-IRES-Fluc was transfected into Huh7 cells. The cells were cultured in the presence of the indicated concentrations of compounds 1 through 4. After 6 h of treatment, luciferase activities were measured, and the values were normalized against *Renilla* luciferase activities. The assays were performed in triplicate. The bars indicate means and SD.

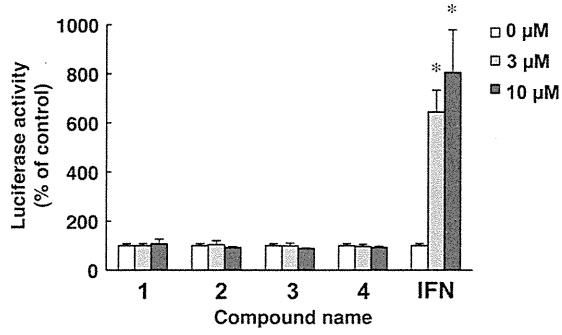

FIG 3 Hit compounds do not activate interferon-stimulated gene responses. Plasmids pISRE-TA-Luc and pRL-CMV were cotransfected into Huh7 cells. The transfected cells were cultured in the presence of the indicated concentrations of the hit compounds. After 6 h of treatment, luciferase activities were measured, and the values were normalized against *Renilla* luciferase activities. As positive controls, cells were treated with IFN-α at a concentration of 0, 3, or 10 U/ml. The bars indicate means and SD. The asterisks indicate *P* values of less than 0.01.

Hit compounds do not activate interferon-stimulated gene responses. To study whether the actions of the hit compounds involved IFN-mediated antiviral signaling that would induce expression of an IFN-stimulated gene, an ISRE-luciferase reporter plasmid, pISRE-TA-Luc, was transfected into Huh7 cells, and the transfected cells were cultured in the presence of the 4 compounds at concentrations of 0, 3, or 10 μM. In contrast to interferon, which elevated ISRE promoter activities significantly, the hit compounds showed no effects on the ISRE-luciferase activities (Fig. 3). These results indicated that the action of the hit compounds is independent of interferon signaling.

Drug synergism with IFN-α or BILN 2061. To investigate whether the hit compounds were synergistic with IFN-α or the protease inhibitor BILN 2061, we used isobologram analyses (24, 28). HCV replicon cells were treated with a combination of IFN-α or BILN 2061 and each hit compound at an EC_{50} ratio of 1:0. 4:1, 3:2, 2:3, 1:4, or 0:1, and the dose-effect results were plotted (Fig. 4A and C). The fractional EC_{50}s for IFN-α or BILN 2061 and each compound were plotted on the *x* and *y* axes, respectively, to generate an isobologram. As shown in Fig. 4B, all plots of the fractional EC_{50}s of compound 1 and IFN-α fell below the line of additivity, while the plots were located closed to the line of additivity for the treatments using IFN-α plus compound 2 or 3 and above the line for the treatment using IFN-α plus compound 4. Those results indicated that the anti-HCV effect of compound 1 was synergistic with IFN-α, the anti-HCV effects of compounds 2 and 3 were additive, and the effect of compound 4 was antagonistic. In the BILN 2061 combination study, the combination with compound 2 was slightly synergistic, while the combination with compound 1 or 3 was additive, and the combination with compound 4 was antagonistic (Fig. 4D).

SARs of compound 1 and similar compounds. We next conducted SAR analyses for hit compound 1 by screening 69 compounds with structures similar to that of compound 1 (see Table S2 in the supplemental material). Out of those compounds, we identified 4 structural analogues that suppressed subgenomic HCV replication with EC_{50}s ranging from 1.82 to 4.03 μM and SIs of 6.01 through >43.7 (Table 2 and Fig. 5A and B). Similarly, the 4 compounds designated 5, 6, 7, and 8 substantially decreased HCV-NS5A protein expression levels following treatment with the compounds (Fig. 5C). Consistent with the replicon results, the compounds significantly suppressed HCV-JFH1 mRNA in cell culture (Fig. 5D). Although the suppressive activities of the 4 compounds were similar, the original compound 1 showed the greatest anti-HCV activity. Therefore, we conducted SAR analyses of the compound 1 *N*-(morpholine-4-carbonyloxy) amidine and *N*-acyloxy-1-naphthalenacetamidine moieties. We screened 13 compounds containing *N*-(morpholine-4-carbonyloxy) amidine and 11 with *N*-acyloxy-1-naphthalenacetamidine (Fig. 6A; see Table S3 in the supplemental material). Intriguingly, 11 out of the 13 *N*-(morpholine-4-carbonyloxy) amidine compounds suppressed the subgenomic HCV replicon without cytotoxicity at a fixed concentration of 5 μM. In contrast, only 2 *N*-acyloxy-1-naphthalenacetamidine compounds decreased HCV replication (Fig. 6B and C). We also conducted dose-dependent suppression assays for HCV replicon. As shown in Table 3, 11 out of 13 *N*-(morpholine-4-carbonyloxy) amidine compounds consistently decreased subgenomic HCV replication, with EC_{50}s ranging from 1.52 through 8.62 μM and SIs of 14.2 to >61.4. Of these 11 compounds, compound 14 was the most potent, with an EC_{50} of 1.63 μM and an SI of >61.4. The antiviral effect of compound 14 against HCV-JFH1 was identical to that of the original compound 1. To identify the moiety conferring anti-HCV activity, we tested the morpholine-4-carboxyl moiety within the *N*-(morpholine-4-carboynloxy) amidine structure (Fig. 6D). Three compounds bearing the morpholine-4-carboxyl moiety were tested, and none showed suppressive activity toward the HCV replicon. These results suggested that the entire *N*-(morpholine-4-carbonyloxy) amidine moiety was important for efficient anti-HCV activity.

Effect of compound 1 on the NF-κB signaling pathway. NF-κB, composed of homo- and heterodimeric complexes of Rel-like domain-containing proteins, including p50 and p65, is a key regulator of innate and adaptive immune responses through transcriptional activation of several antiviral proteins (9, 23). We performed luciferase reporter assays, a p65 phosphorylation assay, and an IκB-α degradation assay to assess the effect of compound 1 on NF-κB signaling in host cells. Intriguingly, treatment of both Huh7 cells and HCV replicon-expressing cells with compound 1 increased NF-κB reporter activity in a dose-dependent manner (Fig. 7A and B). Consistently, treatment with compound 1 increased phosphorylated NF-κB p65 in Huh7 cells (Fig. 7C). Acti-

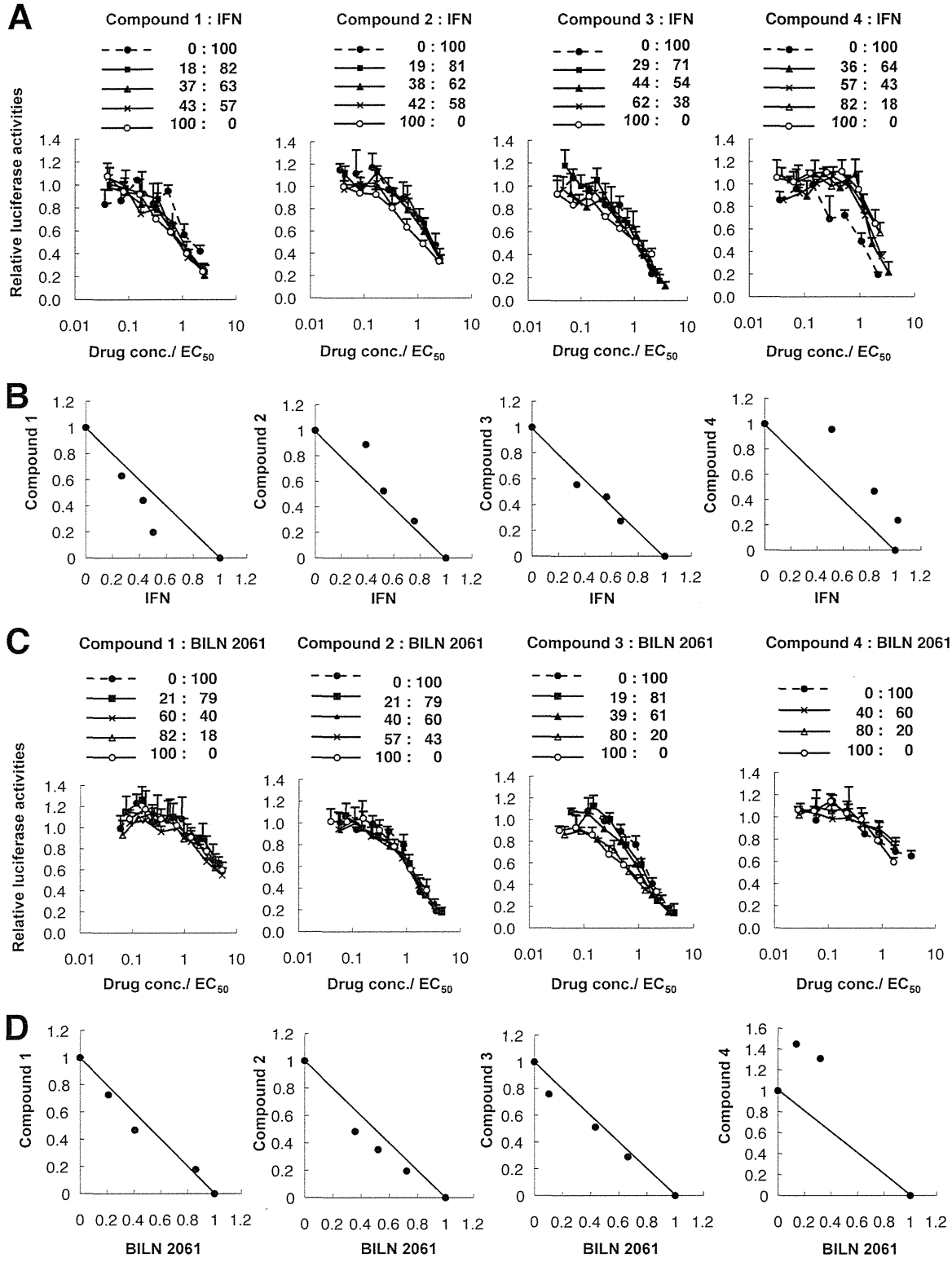

FIG 4 Drug synergism analyses: effects of each of the 4 antiviral hit compounds combined with IFN-α or BILN 2061 on HCV replication. (A and C) Huh7/Rep-Feo cells were cultured with a combination of IFN-α or BILN 2061 and antiviral hit compound 1, 2, 3, or 4 at the indicated ratios, adjusted by the EC_{50} of the individual drug. The internal luciferase activities were measured after 48 h of culture. Assays were performed in triplicate. Shown are means and SD. (B and D) Graphical presentations of isobologram analyses. For each drug combination in panels A and C, the EC_{50}s of IFN-α or BILN 2061 and compound 1, 2, 3, or 4 for inhibition of HCV replication were plotted against the fractional concentrations of IFN-α or BILN 2061 and each compound, as indicated on the x and y axis, respectively. A theoretical line of additivity is drawn between the EC_{50}s for each drug alone.

TABLE 2 Effects of derivative compounds of 1 on HCV replication[a]

Compound	EC_{50} (μM)	CC_{50} (μM)	SI
5	1.82 (0.58–5.68)	45.1 (14.3–52.5)	24.8
6	2.29 (1.57–3.34)	>100	>43.7
7	2.83 (1.43–5.78)	17.0 (5.25–38.7)	6.01
8	4.03 (3.51–4.63)	87.8 (59.1–172)	21.8

[a] The EC_{50} and CC_{50} values are reported, with 95% confidence intervals in parentheses, from a representative experiment performed in triplicate.

vation of NF-κB involves degradation of a suppressor protein, IκB-α. As shown in Fig. 7D, IκB-α protein levels were strongly decreased in cells treated with compound 1. Additionally, activation of the NF-κB pathway by TNF-α treatment significantly suppressed HCV replication (Fig. 7E). These results indicated that the antiviral action of compound 1 partially involved activation of the NF-κB signaling pathway.

DISCUSSION

Using a chimeric luciferase reporter-based subgenomic HCV-Feo replicon assay and an HCV-JFH1 cell culture, we discovered 4 novel anti-HCV compounds from cell-based screening of a library of 4,004 chemicals (Fig. 1 and Table 1). These compounds displayed anti-HCV activity at noncytotoxic concentrations. The most potent of the leading hit compounds was MCNA, and SAR analyses revealed that 4 compounds with structures similar to that of MCNA also had antiviral activity (Fig. 5). Furthermore, we showed that the *N*-(morpholine-4-carbonyloxy) amidine moiety within the structure of MCNA is essential for antiviral activity (Fig. 6).

After the development of the HCV replicon system, the study of HCV replication and discovery of novel anti-HCV agents have shown great progress. To date, our group and others have already made several successful attempts to discover novel inhibitors of HCV replication. Using Huh7/Rep-Feo cells, we previously identified novel anti-HCV substances, including cyclosporins (18, 19), short interfering RNA (siRNA) (31), hydroxyl-methyl-glutaryl coenzyme A reductase inhibitors (10), and epoxide compounds (20). Huh7/Rep-Feo cells were also used for screening a whole-genome siRNA library and successfully identified human genes that support HCV replication (27). Although the HCV replicon system cannot screen for inhibitors of viral entry and release, it is still a useful tool for rapid, reliable, and reproducible high-throughput screening. In our study, we used library sets of compounds that had probably not been used for anti-HCV drug screening before.

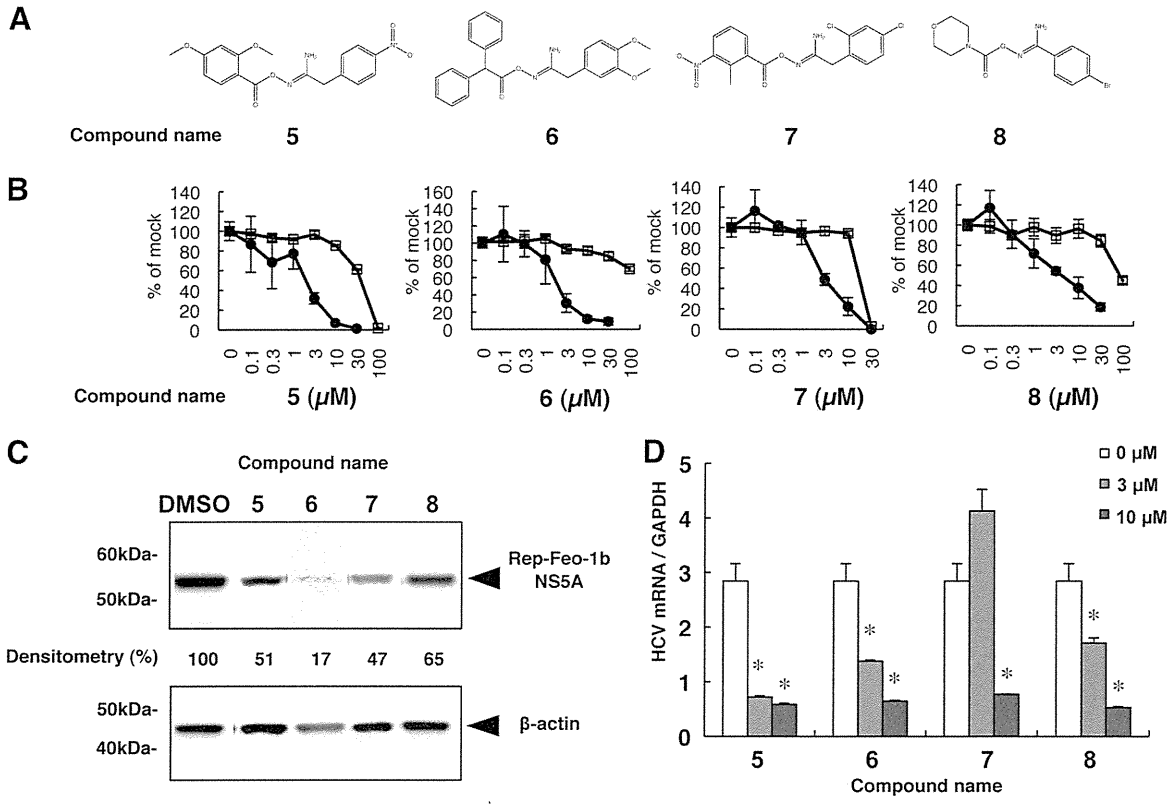

FIG 5 Effects of derivatives of compound 1 on HCV replication. (A) Chemical structures of screening hits of compound 1 derivatives. (B) Huh7/Rep-Feo cells were treated with various concentrations of each compound for 48 h. Luciferase activity for HCV RNA replication is shown as a percentage of the DMSO-treated control luciferase activity (solid circles). Cell viability is also shown as a percentage of control viability (open squares). Each point represents the mean of triplicate data points, with standard deviations represented as error bars. (C) HCV NS5A protein expression levels in Huh7/Rep-Feo cells after treatment with the hit compounds. Huh7/Rep-Feo cells were treated with DMSO and derivative compounds at 5 μM for 48 h, and Western blotting was performed using anti-HCV NS5A and anti-β-actin antibodies. Densitometry of the NS5A protein was performed, and the results are indicated as percentages of the DMSO-treated control. The assay was repeated three times, and a representative result is shown. (D) Huh7.5.1 cells were transfected with HCV-JFH1 RNA and cultured in the presence of the indicated compounds at a concentration of 3 μM or 10 μM. At 72 h after transfection, total cellular RNA was extracted, followed by real-time RT-PCR. The bars indicate means and SD. The asterisks indicate *P* values of less than 0.01. GAPDH, glyceraldehyde-3-phosphate dehydrogenase.

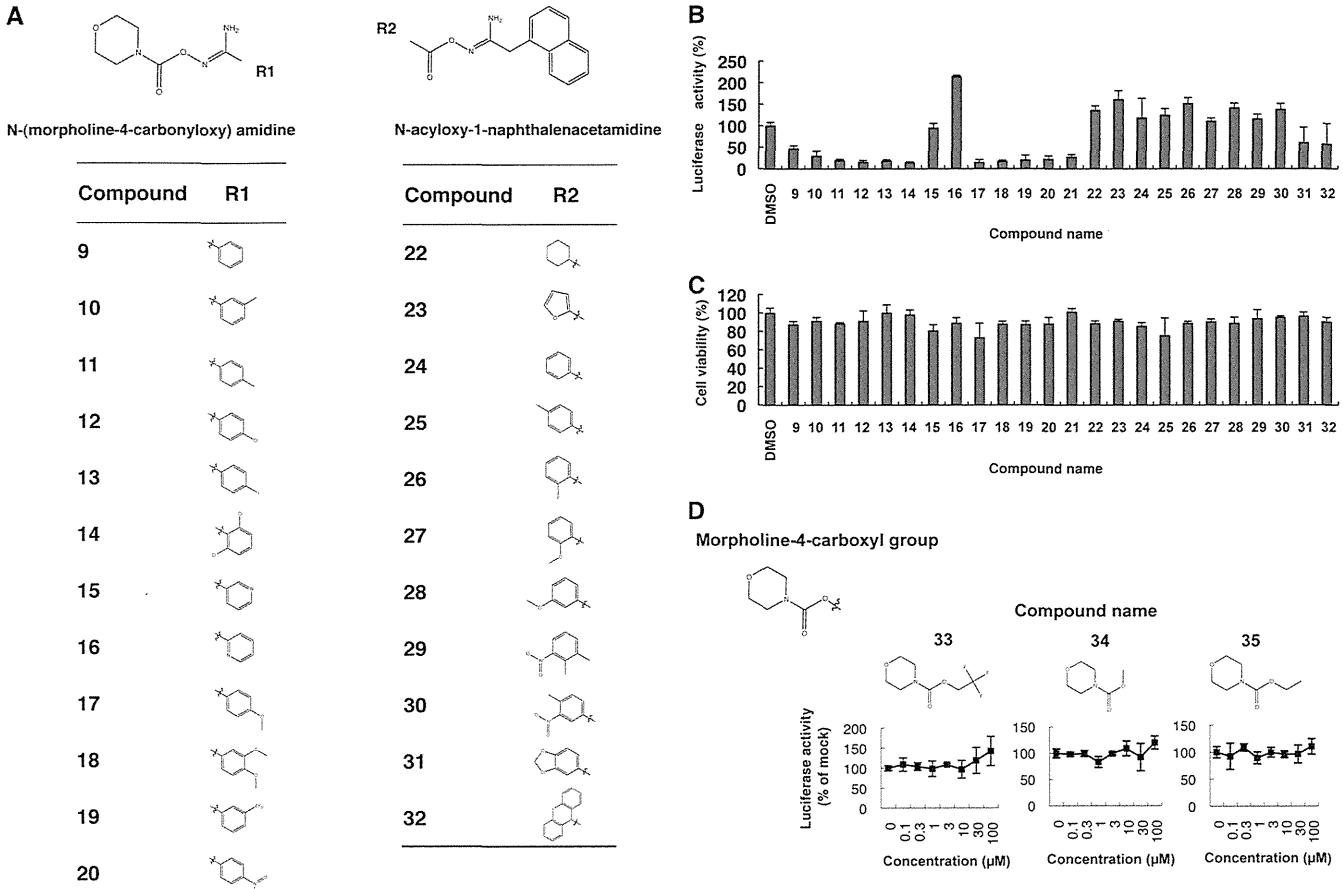

FIG 6 SARs of derivatives of compound 1 that contain *N*-(morpholine-4-carbonyloxy) amidine or *N*-acyloxy-1-naphthalenacetamidine moieties. (A) Chemical structures of compounds with *N*-(morpholine-4-carbonyloxy) amidine or *N*-acyloxy-1-naphthalenacetamidine analyzed for SARs. (B) Huh7/Rep-Feo cells were cultured in the presence of 13 compounds with *N*-(morpholine-4-carbonyloxy) amidine and 11 compounds with *N*-acyloxy-1-naphthalenacetamidine at a fixed concentration of 5 μM. The internal luciferase activities were measured after 48 h of culture. Luciferase activity for HCV RNA replication levels is shown as a percentage of the drug-negative (DMSO) control. Assays were performed in triplicate. The bars indicate means and SDs. (C) Cell viability is shown as a percentage of control viability. Assays were performed in triplicate. The bars indicate means and SD. (D) Effects of morpholine-4-carboxyl compounds on HCV replication. Huh7/Rep-Feo cells were treated with various concentrations of compound 33, 34, or 35 for 48 h. Luciferase activity for HCV RNA replication levels is shown as a percentage of the drug-negative (DMSO) control. Each point represents the mean of triplicate data points, with standard deviations represented as error bars.

TABLE 3 Effects of *N*-(morpholine-4-carbonyloxy) amidine compounds on HCV replication[a]

Compound	EC_{50} (μM)	CC_{50} (μM)	SI
9	8.62 (7.03–10.6)	>100	>11.1
10	3.32 (2.28–4.84)	47.0 (15.7–76.4)	14.2
11	1.55 (1.04–2.30)	48.8 (12.8–95.6)	31.5
12	1.52 (1.14–2.02)	51.0 (16.2–96.7)	33.6
13	1.60 (1.36–1.88)	38.6 (29.4–50.7)	24.1
14	1.63 (1.34–2.00)	>100	>61.4
15	ND	ND	ND
16	ND	ND	ND
17	1.77 (1.39–2.26)	63.3 (21.8–128)	35.8
18	3.80 (2.48–5.83)	100 (86.8–138)	26.3
19	1.99 (1.59–2.48)	55.1 (14.8–105)	27.7
20	2.61 (1.68–4.05)	>100	>38.3
21	1.55 (1.45–1.67)	94.6 (93.0–98.0)	61.0

[a] The EC_{50} and CC_{50} values are reported, with 95% confidence intervals in parentheses, from a representative experiment performed in triplicate. ND, not determined.

The morpholine moiety is a common pharmacophore present in many biosynthetic compounds, such as antimycotic agents (4, 21), and inhibitors of phosphoinositide 3-kinases (5, 16, 30), TNF-α-converting enzymes (14), and matrix metalloproteinases (1). Among the antimycotic morpholine derivatives, amorolfine has been widely used to treat onychomycosis (4, 21). The morpholino oxygen in a synthetic phosphoinositide 3-kinase inhibitor, LY294002, participated directly in a key hydrogen-bonding interaction at the ATP-binding site of phosphoinositide 3-kinase γ (30). Although the morpholine moieties are key components of many inhibitors, anti-HCV morpholine compounds have not yet been reported. In this report, we demonstrated for the first time that a morpholine-bearing compound, *N*-(morpholine-4-carbonyloxy) amidine, had a potent antiviral effect on HCV replication.

Among the 4 hit compounds, MCNA activated the NF-κB pathway (Fig. 7A, B, C, and D). NF-κB is a central regulator of innate and adaptive immune responses. NF-κB-induced tran-

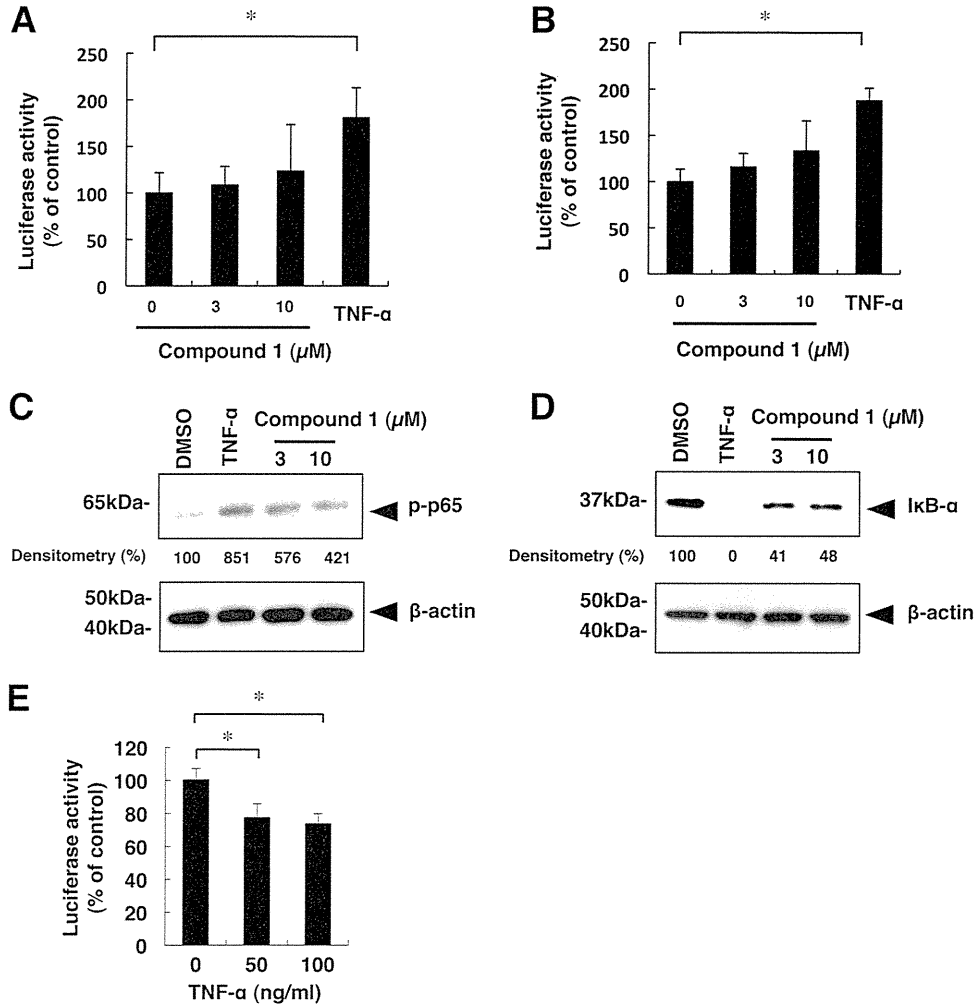

FIG 7 Effects of compound 1 on the NF-κB signaling pathway. (A and B) NF-κB-responsive luciferase reporter assays. The plasmids pNF-κB-TA-Fluc and pRL-CMV were cotransfected into Huh7 cells (A) or HCV replicon-expressing cells (B). At 24 h after transfection, cells were treated with compound 1 at a concentration of 0, 3, or 10 μM. After 6 h, luciferase activities were measured, and the values were normalized against *Renilla* luciferase activities. As a positive control, cells were treated with TNF-α (50 ng/ml). Assays were performed in triplicate. The bars indicate means and SD. (C and D) Huh7 cells were treated for 30 min with compound 1 at concentrations of 3 and 10 μM, and Western blot analyses of phosphorylated p65 and IκBα were conducted. As a positive control, cells were treated with TNF-α (50 ng/ml). β-Actin served as a loading control. Densitometry of phosphorylated p65 protein and IκB-α protein was performed, and the results are indicated as percentages of the DMSO-treated control. The assay was repeated three times, and a representative result is shown. (E) Effect of activation of NF-κB signaling on HCV RNA replication. Huh7/Rep-Feo cells were treated with TNF-α at a concentration of 0, 50, or 100 ng/ml for 48 h. Luciferase activity for HCV RNA replication levels is shown as a percentage of untreated negative-control luciferase activity. Assays were performed in replicates of 6. The asterisks indicate *P* values of less than 0.01.

scription is induced in response to a variety of signals, including proinflammatory cytokines, stress induction, and by-products of microbial and viral infection (9). In HCV-infected cells, activation of transcription factors, such as NF-κB and many interferon regulatory factors, proceeds mainly through Toll-like receptors and RIG-I-dependent host signaling pathways triggered by double-stranded RNA products (3). NF-κB, interferon regulatory factor 1, and interferon regulatory factor 3 bind to the positive regulatory domains of the IFN-β promoter to induce IFN-β expression and elicit antiviral states in host cells (23). Therefore, we hypothesized that the augmentation of host antiviral response through NF-κB activation is an important strategy for anti-HCV treatment. Our demonstration that the activation of NF-κB signaling suppressed HCV replication appears to follow this strategy (Fig. 7E). In support of the idea, Toll-like receptor 7 agonist has shown anti-HCV effects in a preclinical study (7). The anti-HCV activities of MCNA cannot be explained solely by NF-κB activation, because its antiviral activity was much more potent than selective NF-κB activation by TNF-α treatment (Fig. 7E). There remains the possibility that MCNA has a direct viral target. It will be important to assess whether long-term exposure to the compounds could select resistant variants. Although other mechanisms may underlie the antiviral activity, we hypothesize that one of the antiviral mechanisms of MCNA is NF-κB activation that is independent of IFN signaling.

Although several DAAs are currently in advanced clinical trials and the recently approved telaprevir and boceprevir combination therapies achieved high sustained virologic response rates, the frequent emergence of drug-resistant viruses is a major weakness of such agents. An ongoing search for more potent

and less toxic antiviral agents to improve anti-HCV chemotherapeutics is necessary. Our results indicate that MCNA and related *N*-(morpholine-4-carbonyloxy) amidine compounds constitute a new class of anti-HCV agents. Additional investigations elucidating their mechanism of action, and future modifications to improve anti-HCV activity, may open a new anti-HCV therapeutic window.

ACKNOWLEDGMENTS

We thank Frank Chisari for providing Huh7.5.1 cells, Takaji Wakita for providing the plasmid pJFH1full, and the Chemical Biology Screening Center of Tokyo Medical and Dental University for their assistance in this work.

This study was supported in part by grants from the Ministry of Education, Culture, Sports, Science and Technology of Japan; the Japan Society for the Promotion of Science, Ministry of Health, Labor and Welfare; the Japan Health Sciences Foundation; and the National Institute of Biomedical Innovation.

We declare that we have nothing to disclose regarding funding from industries or conflicts of interest with respect to the manuscript.

REFERENCES

1. **Almstead NG, et al.** 1999. Design, synthesis, and biological evaluation of potent thiazine- and thiazepine-based matrix metalloproteinase inhibitors. J. Med. Chem. 42:4547–4562.
2. **Bailey M, Williams NA, Wilson AD, Stokes CR.** 1992. PROBIT: weighted probit regression analysis for estimation of biological activity. J. Immunol. Methods 153:261–262.
3. **Bigger CB, et al.** 2004. Intrahepatic gene expression during chronic hepatitis C virus infection in chimpanzees. J. Virol. 78:13779–13792.
4. **Flagothier C, Piérard-Franchimont C, Piérard GE.** 2005. New insights into the effect of amorolfine nail lacquer. Mycoses 48:91–94.
5. **Hickson I, et al.** 2004. Identification and characterization of a novel and specific inhibitor of the ataxia-telangiectasia mutated kinase ATM. Cancer Res. 64:9152–9159.
6. **Hoofnagle JH, Seeff LB.** 2006. Peginterferon and ribavirin for chronic hepatitis C. N. Engl. J. Med. 355:2444–2451.
7. **Horsmans Y, et al.** 2005. Isatoribine, an agonist of TLR7, reduces plasma virus concentration in chronic hepatitis C infection. Hepatology 42:724–731.
8. **Kanazawa N, et al.** 2004. Regulation of hepatitis C virus replication by interferon regulatory factor 1. J. Virol. 78:9713–9720.
9. **Karin M, Lin A.** 2002. NF-kappaB at the crossroads of life and death. Nat. Immunol. 3:221–227.
10. **Kim SS, et al.** 2007. A cell-based, high-throughput screen for small molecule regulators of hepatitis C virus replication. Gastroenterology 132: 311–320.
11. **Kwo PY, et al.** 2010. Efficacy of boceprevir, an NS3 protease inhibitor, in combination with peginterferon alfa-2b and ribavirin in treatment-naive patients with genotype 1 hepatitis C infection (SPRINT-1): an open-label, randomised, multicentre phase 2 trial. Lancet 376:705–716.
12. **Kwong AD, Kauffman RS, Hurter P, Mueller P.** 2011. Discovery and development of telaprevir: an NS3-4A protease inhibitor for treating genotype 1 chronic hepatitis C virus. Nat. Biotechnol. 29:993–1003.
13. **Lauer GM, Walker BD.** 2001. Hepatitis C virus infection. N. Engl. J. Med. 345:41–52.
14. **Levin JI, et al.** 2005. Acetylenic TACE inhibitors. Part 2: SAR of six-membered cyclic sulfonamide hydroxamates. Bioorg. Med. Chem. Lett. 15:4345–4349.
15. **Lipinski CA, Lombardo F, Dominy BW, Feeney PJ.** 2001. Experimental and computational approaches to estimate solubility and permeability in drug discovery and development settings. Adv. Drug Deliv. Rev. 46:3–26.
16. **Menear KA, et al.** 2009. Identification and optimisation of novel and selective small molecular weight kinase inhibitors of mTOR. Bioorg. Med. Chem. Lett. 19:5898–5901.
17. **Mishima K, et al.** 2010. Cell culture and in vivo analyses of cytopathic hepatitis C virus mutants. Virology 405:361–369.
18. **Nakagawa M, et al.** 2004. Specific inhibition of hepatitis C virus replication by cyclosporin A. Biochem. Biophys. Res. Commun. 313:42–47.
19. **Nakagawa M, et al.** 2005. Suppression of hepatitis C virus replication by cyclosporin A is mediated by blockade of cyclophilins. Gastroenterology 129:1031–1041.
20. **Peng LF, et al.** 2007. Identification of novel epoxide inhibitors of hepatitis C virus replication using a high-throughput screen. Antimicrob. Agents Chemother. 51:3756–3759.
21. **Polak A, Jäckel A, Noack A, Kappe R.** 2004. Agar sublimation test for the in vitro determination of the antifungal activity of morpholine derivatives. Mycoses 47:184–192.
22. **Poordad F, et al.** 2011. Boceprevir for untreated chronic HCV genotype 1 infection. N. Engl. J. Med. 364:1195–1206.
23. **Randall RE, Goodbourn S.** 2008. Interferons and viruses: an interplay between induction, signalling, antiviral responses and virus countermeasures. J. Gen. Virol. 89:1–47.
24. **Sakamoto N, et al.** 2007. Bone morphogenetic protein-7 and interferon-alpha synergistically suppress hepatitis C virus replicon. Biochem. Biophys. Res. Commun. 357:467–473.
25. **Sarrazin C, Zeuzem S.** 2010. Resistance to direct antiviral agents in patients with hepatitis C virus infection. Gastroenterology 138:447–462.
26. **Soothill JS, Ward R, Girling AJ.** 1992. The IC50: an exactly defined measure of antibiotic sensitivity. J. Antimicrob. Chemother. 29:137–139.
27. **Tai AW, et al.** 2009. A functional genomic screen identifies cellular cofactors of hepatitis C virus replication. Cell Host Microbe 5:298–307.
28. **Tanabe Y, et al.** 2004. Synergistic inhibition of intracellular hepatitis C virus replication by combination of ribavirin and interferon-alpha. J. Infect. Dis. 189:1129–1139.
29. **Wakita T, et al.** 2005. Production of infectious hepatitis C virus in tissue culture from a cloned viral genome. Nat. Med. 11:791–796.
30. **Walker EH, et al.** 2000. Structural determinants of phosphoinositide 3-kinase inhibition by wortmannin, LY294002, quercetin, myricetin, and staurosporine. Mol. Cell 6:909–919.
31. **Yokota T, et al.** 2003. Inhibition of intracellular hepatitis C virus replication by synthetic and vector-derived small interfering RNAs. EMBO Rep. 4:602–608.
32. **Zhong J, et al.** 2005. Robust hepatitis C virus infection in vitro. Proc. Natl. Acad. Sci. U. S. A. 102:9294–9299.

Antiviral Therapy 2012; 17:35-43 (doi: 10.3851/IMP1923)

Original article

Age and total ribavirin dose are independent predictors of relapse after interferon therapy in chronic hepatitis C revealed by data mining analysis

*Masayuki Kurosaki[1], Naoki Hiramatsu[2], Minoru Sakamoto[3], Yoshiyuki Suzuki[4], Manabu Iwasaki[5], Akihiro Tamori[6], Kentaro Matsuura[7], Sei Kakinuma[8], Fuminaka Sugauchi[9], Naoya Sakamoto[8], Mina Nakagawa[8], Hiroshi Yatsuhashi[10], Namiki Izumi[1]**

[1]Division of Gastroenterology and Hepatology, Musashino Red Cross Hospital, Tokyo, Japan
[2]Department of Gastroenterology and Hepatology, Osaka University Graduate School of Medicine, Osaka, Japan
[3]First Department of Internal Medicine, University of Yamanashi, Yamanashi, Japan
[4]Department of Hepatology, Toranomon Hospital, Tokyo, Japan
[5]Department of Computer and Information Science, Seikei University, Tokyo, Japan
[6]Department of Hepatology, Osaka City University Medical School, Osaka, Japan
[7]Department of Gastroenterology and Metabolism, Nagoya City University Graduate School of Medical Sciences, Nagoya, Japan
[8]Department of Gastroenterology and Hepatology, Tokyo Medical and Dental University, Tokyo, Japan
[9]Department of Gastroenterology, Nagoya Koseiin Medical Welfare Center, Nagoya, Japan
[10]Clinical Research Center, National Nagasaki Medical Center, Nagasaki, Japan

*Corresponding author e-mail: nizumi@musashino.jrc.or.jp

Background: This study aimed to define factors associated with relapse among responders to pegylated interferon (PEG-IFN) plus ribavirin (RBV) therapy in chronic hepatitis C.

Methods: A cohort of genotype 1b chronic hepatitis C patients treated with PEG-IFN plus RBV and who had an undetectable HCV RNA by week 12 (n=951) were randomly assigned to model derivation (n=636) or internal validation (n=315) groups. An independent cohort (n=598) were used for an external validation. A decision tree model for relapse was explored using data mining analysis.

Results: The data mining analysis defined five subgroups of patients with variable rates of relapse ranging from 13% to 52%. The reproducibility of the model was confirmed by internal and external validations (r^2=0.79 and 0.83, respectively). Patients with undetectable HCV RNA at week 4 had the lowest risk of relapse (13%), followed by patients <60 years with undetectable HCV RNA at week 5–12 who received ≥3.0 g/kg of body weight of RBV (16%). Older patients with a total RBV dose <3.0 g/kg had the highest risk of relapse (52%). Higher RBV dose beyond 3.0 g/kg was associated with further decrease of relapse rate among patients <60 years (up to 11%) but not among older patients whose relapse rate remained stable around 30%.

Conclusions: Data mining analysis revealed that time to HCV RNA negativity, age and total RBV dose was associated with relapse. To prevent relapse, ≥3.0 g/kg of RBV should be administered. Higher dose of RBV may be beneficial in patients <60 years.

Introduction

The currently recommended therapy for chronic hepatitis C is a combination of pegylated interferon (PEG-IFN) plus ribavirin (RBV) [1]. This therapy is effective in 50% of patients with HCV genotype 1b [2,3]. The most reliable predictor of sustained virological response (SVR) is the response during early weeks of therapy. A satisfactory response to therapy in the early weeks is associated with a high rate of SVR [4–8]. A basic concept of response-guided therapy is to modify the duration of therapy according to the time to HCV RNA negativity. Extended therapy may be given to patients with delayed virological response [9–13]. Modification of duration of therapy or drug dose may also be necessary in patients with early virological

response (EVR), because approximately 20% of these patients experience relapse after the completion of 48 weeks of therapy. Recent reports have revealed that single nucleotide polymorphisms located near the *IL28B* gene are strongly associated with SVR or a null response to PEG-IFN plus RBV therapy [14–16]. However, single nucleotide polymorphisms located near the *IL28B* gene are not associated with relapse after EVR [17]. Identification of risk factors for relapse among patients with virological response may lead to more individualized therapy and improved SVR rate.

Decision tree analysis, a core component of data mining analysis, is a method that explores data to develop predictive models [18]. This method has been originally used in business and recently in medical fields [19–25]. Decision tree analysis was successfully used to build a predictive model of EVR [26] and SVR to PEG-IFN plus RBV combination therapy in chronic hepatitis C [17,27,28]. The results of the analysis are presented as a tree structure, which is easy to understand and use in clinical practice. Patients can be allocated into subgroups by simply following the flowchart form of the decision tree [29].

In the present study, we used decision tree analysis to identify predictors of relapse among patients who achieved EVR to PEG-IFN plus RBV therapy, and to define a more individualized therapeutic strategy beyond response-guided therapy.

Table 1. Background of study population

Characteristic	Value
Age, years	54.9 (10.8)
Gender	-
Male, *n* (%)	557 (59)
Female, *n* (%)	394 (41)
Body mass index, kg/m^2	23.2 (3.3)
Albumin, g/dl	4.1 (1.8)
Creatinine, mg/dl	0.7 (0.2)
AST, IU/l	60.6 (46.2)
ALT, IU/l	80.7 (77.2)
GGT, IU/l	52.0 (60.0)
White blood cell count, cells/μl	4,993 (1,363)
Haemoglobin, g/dl	15.9 (52.6)
Platelets, 10^9/l	174.4 (6.1)
HCV RNA, KIU/ml	1,655 (1,455)
Fibrosis stage	-
F1–2, *n* (%)	626 (66)
F3–4, *n* (%)	98 (10)
NA, *n* (%)	227 (24)
Time to HCV RNA negativity 4/8/12 weeks	-
4 Weeks, *n* (%)	233 (24)
8 Weeks, *n* (%)	386 (41)
12 Weeks, *n* (%)	332 (35)
Treatment duration, weeks	42 (13)
Total RBV dose, g/kg body weight	3.1 (1.3)
Total PEG-IFN dose, μg/kg body weight	62.5 (38.6)
Outcome	-
Relapse, *n* (%)	238 (25)
SVR, *n* (%)	713 (75)

Total *n*=951. Data are expressed as mean (sd) unless otherwise indicated. ALT, alanine aminotransferase; AST, aspartate aminotransferase; GGT, γ-glutamyltransferase; NA, not available; PEG-IFN, pegylated interferon; RBV, ribavirin; SVR: sustained virological response.

Methods

Patients

This is a multicentre retrospective cohort study involving Musashino Red Cross Hospital, Toranomon Hospital, Tokyo Medical and Dental University, Osaka University, Nagoya City University, Yamanashi University, Osaka City University, and their related hospitals. The inclusion criteria were chronic hepatitis C patients treated with PEG-IFN-α2b plus RBV, genotype 1b, pretreatment HCV RNA titre >100 KIU/ml as confirmed by quantitative PCR; Cobas Amplicor HCV Monitor version 2.0; Roche Diagnostic Systems, Pleasanton, CA, USA), an undetectable HCV RNA level within week 12 after the start of therapy, no coinfection with HBV or HIV, and no other causes of liver disease. Patients were treated with PEG-IFN-α2b (1.5 μg/kg) subcutaneously every week plus a daily weight-adjusted RBV dose (600 mg for patients weighing <60 kg, 800 mg for patients weighing 60–80 kg and 1,000 mg for patients weighing >80 kg). Dose reduction or discontinuation of PEG-IFN and RBV was considered based on the recommendations of the package inserts and the discretion of physicians at each university and hospital. The standard duration of therapy was set at 48 weeks, but extension of duration was allowed and implemented at the discretion of each physician. The duration of therapy was extended beyond 48 weeks in 118 patients (mean duration was 56.3 weeks, ranging from 49 to 72 weeks). Although the exact reason for the prolonged treatment in each case was not available, one reason may be that each physician tried to achieve high adherence of RBV by extending the duration of therapy. Another reason may be the late time point of HCV RNA negativity even within early virological response. Among 118 patients, time to HCV RNA negativity was between 9 to 12 weeks in 56% of patients.

A total of 951 patients fulfilled the study criteria. The baseline characteristics and representative laboratory test results are listed in Table 1. For analysis, patients were randomly assigned to either the model derivation (636 patients) or internal validation (315 patients) groups. There were no significant differences in the clinical backgrounds between these two groups. For external validation of the model, we collaborated with another multicentre study group consisting of 29 medical centres and hospitals belonging to the National

Hospital Organization (Japan). A dataset collected from 598 patients who were treated with PEG-IFN-α2b plus RBV and had undetectable HCV RNA within week 12 were used for external validation. Informed consent was obtained from each patient. The study protocol conformed to the ethical guidelines of the Declaration of Helsinki and was approved by the institutional review committees of all concerned hospitals.

Laboratory tests

Haematological tests, blood chemistry and HCV RNA titre were analysed before therapy and at least once every month during therapy. Rapid virological response (RVR) was defined as an undetectable HCV RNA level at week 4, and complete early virological response (cEVR) was defined as an undetectable HCV RNA level at week 5 through week 12 after the start of therapy. SVR was defined as an undetectable HCV RNA level 24 weeks after the completion of therapy. Detection of HCV RNA level was based on qualitative PCR with a lower detection limit of 50 IU/ml (Amplicor; Roche Diagnostic Systems). A database of pretreatment variables included haematological tests (haemoglobin level, white blood cell count and platelet count), blood chemistry tests (serum levels of creatinine, albumin, aspartate aminotransferase, alanine aminotransferase, γ-glutamyltransferase, total cholesterol, triglycerides and HCV RNA titre), stage of histological fibrosis and patient characteristics (age, sex and body mass index). Post-treatment variables included time to HCV RNA negativity, calculated total RBV dose (g/kg of body weight), and calculated total PEG-IFN dose (μg/kg of body weight).

Statistical analysis

The Student's *t*-test was used for the univariable comparison of quantitative variables and Fisher's exact test was used for the comparison of qualitative variables. Logistic regression models with backward selection procedures were used for multivariable analysis of factors associated with relapse. IBM SPSS software version 18.0 (SPSS Inc., Chicago, IL, USA) was used for analysis. For the decision tree analysis [30], the data mining software IBM SPSS Modeler 14 (SPSS Inc.) was used, as reported previously [17,26–28]. The decision tree analysis, the core component of the data mining, belongs to a family of non-parametric regression methods based on binary recursive partitioning of data. In this analysis, the software automatically explored the database to determine optimal split variables to build a decision tree structure. A statistical search algorithm evaluate the model derivation group to determine the optimum variables and cutoff values and to yield the most significant division of patients into two subgroups that were as homogeneous as possible for the probability of relapse. Once patients were divided into 2 subgroups, the analysis was automatically repeated on each subgroup in the same way until either no additional significant variable was detected or the number of patients was <20. Finally all patients were classified into particular subgroups that are homogeneous with respect to the probabilities of relapse.

Results

The decision tree model for the prediction of relapse

The overall rate of relapse was 26% in the model derivation group. The decision tree analysis selected three variables that are associated with relapse: time to HCV RNA negativity, age and total RBV dose (Figure 1). Time to HCV RNA negativity was selected as the best predictor of relapse. The rate of relapse was 13% for patients with RVR compared to 30% for patients with cEVR. Among patients with cEVR, age was selected as the variable of second split. Patients <60 years had a lower probability of relapse (22%) compared with those ≥60 years (41%). The total RBV dose was selected as the third variable of split with an optimal cutoff of 3.0 g/kg of body weight. The rate of relapse was lower in patients who received ≥3.0 g/kg of body weight of RBV compared to patients who received <3.0 g/kg of body weight (among patients <60 years rates were 16% versus 32% and among patients ≥60 years rates were 26% versus 52%, respectively).

According to this decision tree, the patients were divided into five groups with different rates of relapse ranging from 13% to 52%. Patients with RVR had the lowest risk of relapse. Among patients with cEVR, patients <60 years who received ≥3.0 g/kg of body weight of RBV also had a low risk of relapse (16%). By contrast, patients who received <3.0 g/kg of body weight of RBV had higher than the average risk of relapse, especially in patients ≥60 years (52%).

Validation of the decision tree model

The decision tree model was validated using an internal validation group that was not included in the model derivation. The rates of relapse for each subgroup of patients were correlated closely between the model derivation and the internal validation group (r^2=0.79; Figure 2A). When validated using an external validation group, the rates of relapse for each subgroup of patients were again correlated closely between the model derivation and the external validation group. (r^2=0.83; Figure 2B).

Multivariable logistic regression analysis for factors associated with relapse

Univariable and multivariable analysis was performed using the combined population of model derivation and internal validation group. Univariable analysis found

that age, sex, serum levels of creatinine, haemoglobin, platelet count, HCV RNA titre, time to HCV RNA negativity, total PEG-IFN dose and total RBV dose were associated with relapse. Duration of therapy was not associated with reduction in relapse rate. Multivariable analysis including these factors showed that age, total RBV dose, serum level of creatinine, and time to HCV RNA negativity were independent predictors of relapse (Table 2). Creatinine was not selected as a splitting variable in data mining analysis probably due to the limitation to stop the analysis when the number of patients was <20. Using the combined population of model derivation and internal validation group, patients in each subgroup of decision tree model were further stratified by creatinine levels and the effect of creatinine level on relapse was analysed. Among patients with RVR, the rate of relapse did not differ between patients with creatinine levels of <0.7 g/dl and ≥0.7 g/dl and were 12% and 12%, respectively. Among patients with cEVR, the rate of relapse was higher in patients with creatinine levels of <0.7 g/dl compared to those with creatinine levels of ≥0.7 g/dl and were 39% versus 23%, respectively, for patients <60 years who received <3.0 g/kg of body weight of RBV, 19% versus 14% for patients <60 years who received ≥3.0 g/kg of body weight of RBV, 58% versus 41% for patients ≥60 years who received <3.0 g/kg of body weight of RBV, and 42% versus 26% for patients ≥60 years who received ≥3.0 g/kg of body weight of RBV.

Effect of age and total RBV dose on relapse among patients with cEVR

The effect of total RBV dose on relapse was analysed among patients with cEVR in a combined group of

Figure 1. The decision-tree model of relapse among patients with rapid virological response or complete early virological response

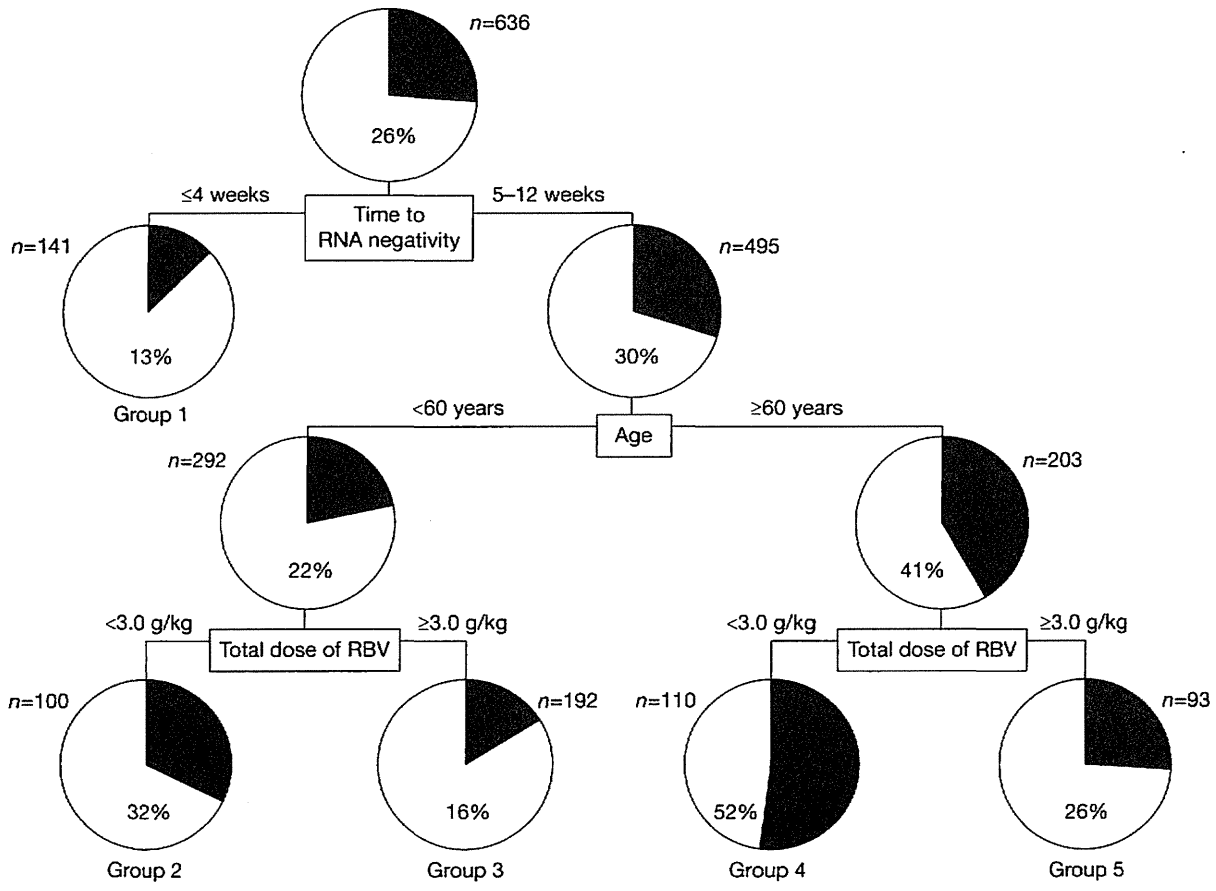

Boxes indicate the factors used for splitting and the cutoff values for the split. Pie charts indicate the rate of relapse for each group of patients after splitting. Terminal groups of patients discriminated by the analysis are numbered from 1 to 5. The rate of relapse was higher than average (>26%) in subgroups 2 and 4, where total ribavirin (RBV) dose was <3 g/kg of body weight.

model derivation and internal validation (n=718). The relapse rate decreased with an increase in RBV dose (Figure 3A). When patients were stratified into two groups according to age, the relapse rate decreased with an increase in RBV dose in patients <60 years. The relapse rate was lowest (11%) in patients <60 years who received ≥4.0 g/kg of body weight of RBV. By contrast, among patients ≥60 years, the relapse rate decreased with an increase in RBV dose up to 3.0 g/kg of body weight, but remained relatively stable despite a further increase in the RBV dose beyond 3.0 g/kg of body weight. The rate of relapse was 31% to 33% in patients who received ≥3.0 g/kg of body weight. Patients ≥60 years had higher relapse rate compared with patients <60 years after stratification by RBV dose (P=0.044 for RBV <2.5 g/kg, P=0.009 for RBV 2.5–2.9 g/kg, P=0.150 for RBV 3.0–3.4 g/kg, P=0.036 for RBV 3.5–3.9 g/kg and P=0.006 for RBV ≥4.0 g/kg).

To exclude the effect of the duration of therapy, patients who received 42–54 weeks of therapy were selected (n=544). Again, the relapse rate decreased with an increase in RBV dose in patients <60 years but remained stable despite a further increase in the RBV dose beyond 3.0 g/kg of body weight in patients ≥60 years (Figure 3B); in addition, patients ≥60 years had a higher relapse rate compared with younger patients after stratification by

Figure 2. Internal and external validation of the decision-tree model: subgroup-stratified comparison of the rate of relapse between the model derivation and validation groups

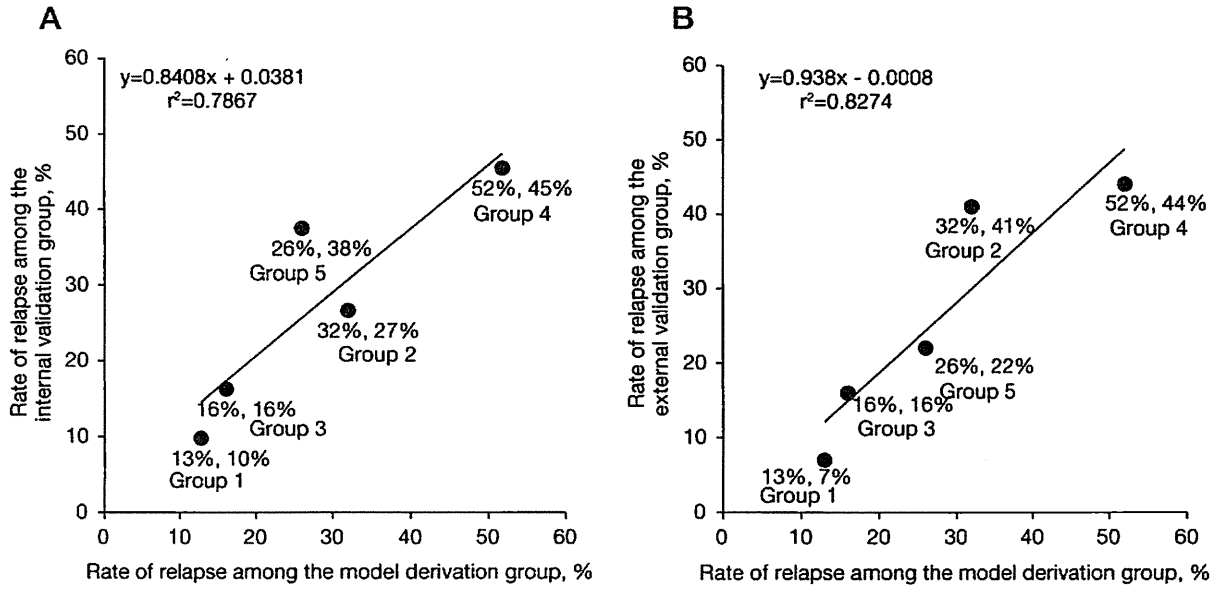

Each patient in the internal and external validation population was allocated to groups 1 to 5 following the flowchart of the decision tree. The rates of relapse were then calculated for each group and a graph was plotted. The rate of relapse in the (A) internal and (B) external validation groups are shown. The rates of relapse are shown as percentages below data points: the value on the left is from the model derivation group and on the right is from the validation group. The rates of relapse in each group of patients correlated closely between the model derivation group and the validation group (correlation coefficient: r^2=0.79 and 0.83, respectively).

Table 2. Multivariable analysis of factors associated with relapse among patients with RVR/cEVR

Factor	OR	95% CI	P-value
No-RVR	4.07	2.57–6.43	<0.0001
Total RBV dose <3.0 g/kg body weight	2.19	1.58 –3.03	<0.0001
Creatinine <0.7 g/dl	1.67	1.22–2.29	0.001
Age ≥60 years	2.37	1.73–3.24	<0.0001

cEVR, complete early virological response (HCV-RNA-positive at week 4, but negative at week 12); RBV, ribavirin; RVR, rapid virological response (HCV-RNA-negative at week 4).